—6—

LITHOSTRATIGRAPHY OF THE CESAR CORES

P.J. Mudie[1] *and S.M. Blasco*[1]
Geological Survey of Canada

Mudie, P.J. and Blasco, S.M., Lithostratigraphy of the CESAR core; in *Initial Geological Report on CESAR — the Canadian Expedition to Study the Alpha Ridge, Arctic Ocean, ed. H.R. Jackson, P.J. Mudie and S.M. Blasco; Geological Survey of Canada, Paper 84-22, p. 59-99, 1985.*

Abstract

Sixteen piston cores and twelve gravity cores were successfully recovered from northern and southern crests of the eastern Alpha Ridge and from the Alpha Ridge graben. All but one core contain late Cenozoic muds with variable amounts of sand- to pebble-sized clastic material that probably reflects transport by ice during the past 4-5 Ma. Sixteen Cenozoic-Holocene lithostratigraphic units have been delimited on the basis of sediment texture, structure, colour, detrital carbonate and authigenic ferromanganese content. The composition of the upper 13 units in the CESAR cores is similar to the Fletcher's Ice Island cores; hence most units can be broadly correlated over most of the Central Arctic Ocean. Three new lithostratigraphic units (A1-A3) occur at the base of CESAR cores from the northern Alpha Ridge crest. Paleomagnetic and palynological data indicate a Late Miocene-Early Pliocene age for unit A3, which confirms previous reports of a slow sedimentation rate during the Cenozoic.

CESAR core 6 was obtained from an erosional surface on top of a fault block at the north edge of the Alpha Ridge graben. This core contains ca. 2m of laminated diatom ooze of Campanian-Maastrichtian age and two ?Paleogene volcanic ash units below a brown mud unit which probably corresponds to units A2 and A3. The biosiliceous ooze contains no foraminifera or silicoflagellates and only few dinoflagellates. There is little difference in biogenic or clastic sediment content between light and dark laminae and the rhythmites do not appear to be annual varves produced in an upwelling environment. The microstructure and fluctuating mineral composition of the laminae most closely resemble those of laminated chert beds in the Triassic forearc basins of Japan.

Résumé

Seize carottes ont été prélevées au moyen d'une carotteuse à piston et douze au moyen d'une carotteuse à chute libre dans les crêtes nord et sud de la partie est de la dorsale Alpha et du graben de la dorsale Alpha. Toutes les carottes sauf une contiennent des boues du Cénozoïque récent ainsi que diverses quantités de matériau clastique dont les dimensions varient de celles du sable à celles du galet et dont la présence reflète vraisemblablement un transport par la glace au cours des quatre ou cinq derniers millions d'années. Seize unités lithostratigraphiques d'âge cénozoïque-holocène sont délimitées en fonction de la texture sédimentaire, la structure, la couleur et le contenu en matériau carbonaté détritique et en ferromanganèse authigène. La composition des treize unités supérieures dans les carottes CESAR s'apparente à celle des carottes qui proviennent de l'île de glace Fletcher et ces unités peuvent être corrélées plus ou moins sur la plus grande partie de l'océan Arctique central. On a décelé la présence de trois nouvelles unités lithostratigraphiques (A1 à A3) à la base des carottes CESAR prélevées dans la crête nord de la dorsale Alpha. Les données paléomagnétiques et palynologiques indiquent que l'unité A3 date du Miocène récent-Pliocène ancien, ce qui confirme que la sédimentation s'est faite lentement au cours du Cénozoïque, conclusion à laquelle avaient abouti d'autres travaux.

[1]Atlantic Geoscience Centre, Bedford Institute of Oceanography, Box 1006, Dartmouth, Nova Scotia, B2Y 4A2

La carotte CESAR 6 provient d'une surface d'érosion situee au-dessus d'un bloc faillé sur la marge nord du graben de la dorsale Alpha. Elle contient environ 2 m de boue de diatomées laminaire qui date du Campanien-Maestrichtien et deux unités de cendres volcaniques du ?Paléogène sous-jacentes à une unité de boue brune correspondant vraisemblablement aux unités A2 et A3. La boue siliceuse de nature organogène ne contient pas de foraminifères ni de silicoflagellés et seulement quelques dinoflagellés. Le contenu en sédiments organogènes ou clastiques varie très peu dans les lamines claires et sombres et les lamines rythmiques ne semblent pas être des varves annuelles produites dans un milieu caractérisé par la remontée des eaux marines. La microstructure et la composition minérale variée des lamines s'apparente étroitement à celles des couches de chert laminaires dans les bassins d'avant-arc triasiques du Japon.

INTRODUCTION

During the Canadian Expedition to Study the Alpha Ridge (CESAR), 28 sediment cores were successfully recovered from the central Arctic Ocean. These cores include the first piston cores taken specifically for sedimentological study of the bathyal Arctic Ocean region. Previous sedimentological studies of this region (Herman, 1974; Clark, 1977; Clark et al., 1980) had to rely on cores taken primarily for geophysical studies; hence, many of these cores were disturbed by sampling or desiccation prior to the commencement of the sediment studies (Clark, 1982). The purposes of this report are to provide the following data on the fresh Arctic Ocean sediment cores: 1) a detailed account of the field and laboratory methods used to obtain, curate and sample the CESAR cores; 2) a description of the lithofacies and their regional correlation; and 3) initial paleoecological interpretion of the lithofacies.

ACKNOWLEDGMENTS

We are grateful to several persons who contributed considerable time to logging the CESAR cores (especially Oliver Maass, Department of Geology, University of Toronto and F.E. Cole, Atlantic Geoscience Centre) and who provided initial biostratigraphic/SEM data (F.E. Cole and B. Deonarine, Atlantic Geoscience Centre). Dr. Patricia Stoffyn (Atlantic Geoscience Centre) has been especially helpful in providing initial geochemical data; W. LeBlanc (Atlantic Geoscience Centre) provided the data for Table 6.3. Several persons provided valuable ideas regarding analysis of the CESAR 6 laminated sediments, particularly Carolyn Isaacs (United States Geological Survey, Menlo Park), Wolfgang Berger and Andy Soutar (Scripps Institute of Oceanography), and David J.W. Piper (Atlantic Geoscience Centre) who also reviewed this paper.

METHODS

Field operations

During CESAR, both piston and gravity coring were possible because the necessary equipment could be transported to the ice camps by C-130 Hercules aircraft. All CESAR piston cores were obtained from the main ice camp; CESAR gravity cores were obtained from both the main camp and the remote camp.

In order to obtain piston cores from the ice platform, in −40°C weather, several modifications of the normal shipboard coring procedures had to be adopted. The required equipment modifications and operational procedures are described in detail by Jodrey and Heffler (1985). Aspects of the coring operations that affected the quality and length of core recovery are outlined below.

The piston corer was constructed from two or three 10ft (3.1m) Benthos core barrels connected by an adapter to a 1200lb (545kg) Alpine core head in order to meet the 550kg weight handling restrictions of the camp and transport facilities. Coring was performed using a standard Benthos split-piston system. Because of the limited size of the hole (1.8 × 1.2 × 2m) that could be kept open for access through the ice, initially a shortened (0.5m) trip arm was used for the trigger weight. CESAR cores 1-3 were obtained with this system; however, the trigger weight frequently became tangled around the main cable and a core head was lost on the fourth attempt. Thereafter, a standard trip-arm length of 1.0m was used for all piston coring. This usually resulted in full corer penetration but the piston always advanced about 60cm above the core sediment and usually less than 3/4ths of the core barrel was filled. A damaged piston valve also reduced the quality of core recovery at sites 2-7; a new valve could not be installed until after recovery of CESAR core 10.

Gravity coring at the main camp was carried out using a light weight corer constructed from a Benthos core head and a 1.5m length of plastic core liner, with an attached corecutter and catcher. CESAR cores 201-211 were obtained by this method which was used successfully for coring on the Lomonosov Ridge (Blasco et al., 1979). At water depths of more than 1475m on the flanks of the northern crest of Alpha Ridge, sediment penetration and core recovery mostly ranged from 44-76cm. At shallower depths, however, less than 10cm of sediment was penetrated and recovered, apparently due to a shallow layer of carbonate-rich "hardgrounds" (*see* CENOZOIC SEDIMENTS). Gravity coring from the mobile camp was performed using a Benthos gravity corer and a 10ft (3.3m) core barrel. This coring system was used to obtain CESAR cores 101-112 from the north side of the southern crest of Alpha Ridge. Penetration ranged from 63-145cm in sediments below the 1475m isobath, and recovery ranged from 9cm at 1490m to 133cm at the deepest site, 1882m. Above the 1475m isobath, penetration ranged from 0-90cm and recovery was 50-100% complete.

Handling and storage of piston cores on CESAR also presented problems due to the confined lab space and very low outdoor temperatures ($-40°$ to $-10°$C). A few sections of CESAR cores 1-6 were lost during derigging operations because of problems during initial attempts to keep the core barrels in a vertical position. The core liners were cut into 1.5m sections and stored vertically in a heated area to prevent freezing and subsequent loss of detailed sediment structure. This procedure was generally successful and freezing only affected small sections of 2 cores: CESAR core 102, at 10cm depth and CESAR core 3, at depths of 110, 130, and 570cm. During transport from the ice camp, the cores were stored vertically in narrow wooden crates and loaded upright into an aircraft cargo-hold which was heated to above freezing.

Table 6.1 lists the locations of the core sites, water depths, and lengths of the sediment recovered. Location of the core sites was controlled by two main logistical con-

Table 6.1 Core numbers, locations, water depths, total length recovered, and time at sediment penetration.

Field number	Latitude °N	Longitude °W	Depth (m)	Length (m)	Day	Time (hr)
CESAR 83-001	85 48.5	110 44.0	2150	5.40	098	1530
" 83-002	85 45.1	110 54.7	1900	6.70	101	0900
" 83-003	85 52.0	109 49.1	1300	7.52	105	2145
" 83-004	85 49.3	109 18.2	1725	4.57	118	1746
" 83-005	85 49.5	109 15.2	1680	3.96	119	2030
" 83-006	85 49.8	109 09.2	1365	3.65	121	1950
" 83-007	85 51.1	108 42.8	1250	3.13	122	2045
" 83-008	85 51.7	108 16.0	1460	4.73	123	2045
" 83-009	85 52.0	108 15.5	1500	5.79	125	0130
" 83-010	85 51.3	108 18.0	1425	4.97	125	2205
" 83-011	85 50.9	108 21.2	1380	5.44	126	2340
" 83-012	85 50.7	108 24.5	1345	5.03	127	2220
" 83-013	85 50.7	108 23.1	1360	5.10	129	0252
" 83-014	85 50.8	108 21.6	1370	4.40	130	0130
" 83-015	85 50.9	108 19.5	1405	4.95	131	1515
" 83-016	85 49.5	108 36.3	1500	3.89	134	2322
Remote camp gravity cores						
CESAR 83-101	85 38.1	111 07.01	1490	0.09	103	1732
" 83-102	85 38.1	111 07.1	1495	1.18	103	1945
" 83-103	85 38.1	110 07.0	1882	1.33	104	0206
" 83-104	85 31.2	110 20.5	1253	0.15	107	2048
" 83-105	85 31.2	110 20.5	1175	0.20	107	2325
" 83-106	85 31.3	110 18.5	1188	0.11	108	1624
" 83-107	85 31.2	110 17.9	1227	0.00	109	ND
" 83-108	85 31.3	110 17.3	1226	0.16	109	1611
" 83-109	85 29.2	110 36.5	1190	0.08	115	0239
" 83-110	85 28.8	110 37.5	1184	0.00	115	1410
" 83-111	85 28.3	110 43.2	1170	0.11	115	2145
" 83-112	85 27.9	110 51.8	1180	0.45	116	1325
Main camp gravity cores						
CESAR 83-201	85 52.4	108 38.8	1533	0.76	110	1655
" 83-202	85 52.2	108 39.2	1585	0.10	111	2103
" 83-203	85 52.3	108 39.7	1480	0.44	112	1620
" 83-204	85 52.2	108 40.2	1475	0.01	113	0330
" 83-205	85 52.2	108 43.2	1400	0.09	113	1557
" 83-206	85 51.9	108 46.1	1400	0.00	113	1900
" 83-207	85 51.9	108 47.0	1375	0.00	113	2040
" 83-208	85 51.3	108 54.5	1188	0.00	114	0550
" 83-209	85 49.5	109 16.2	1690	0.00	116	1640
" 83-210	85 49.5	109 15.2	1680	0.52	117	1420
" 83-211	85 43.9	108 51.9	1730	0.46	118	ND

straints: a) the random direction and speed of the ice camp drift, and b) the time required for setting up the coring operation and re-rigging the corer. The loss of the core head delayed sampling between sites 3 and 4, and coring time was also limited by other demands on winch operation and personnel. Rigging and lowering of the corer took 12 hours and the maximum repetition rate for piston coring was one per 24 hours. The locations of the 16 piston core sites and 14 gravity core sites are shown in Figures 6.1 and 6.2. It should be noted that the water depths for the core sites were measured using echo sounder records corrected for an estimated water sound velocity of 1.47km.s^{-1}; the depths have maximum errors of ca. ±100m. Navigational positioning was determined from four Marconi-761 receivers and is accurate to ±20m.

Laboratory procedures

The crates of CESAR cores were transported to the Atlantic Geoscience Centre (AGC) core facilities where they have been curated and stored in a 4°C refrigerated room. From late June through July 1983, all the cores were split, photographed in colour, X-radiographed, and visually described. At all times during these procedures, great care was taken to avoid contamination of the cores by contact with metal tools or by dust, and to prevent drying or cracking of the sediments. The unsplit core liners were first engraved with the core number and length on 2 sides at the top end. The core liners were then placed in a steel tray to which a precision adjustable router blade was attached, and shallow grooves were cut along the two opposite sides of the core length. The

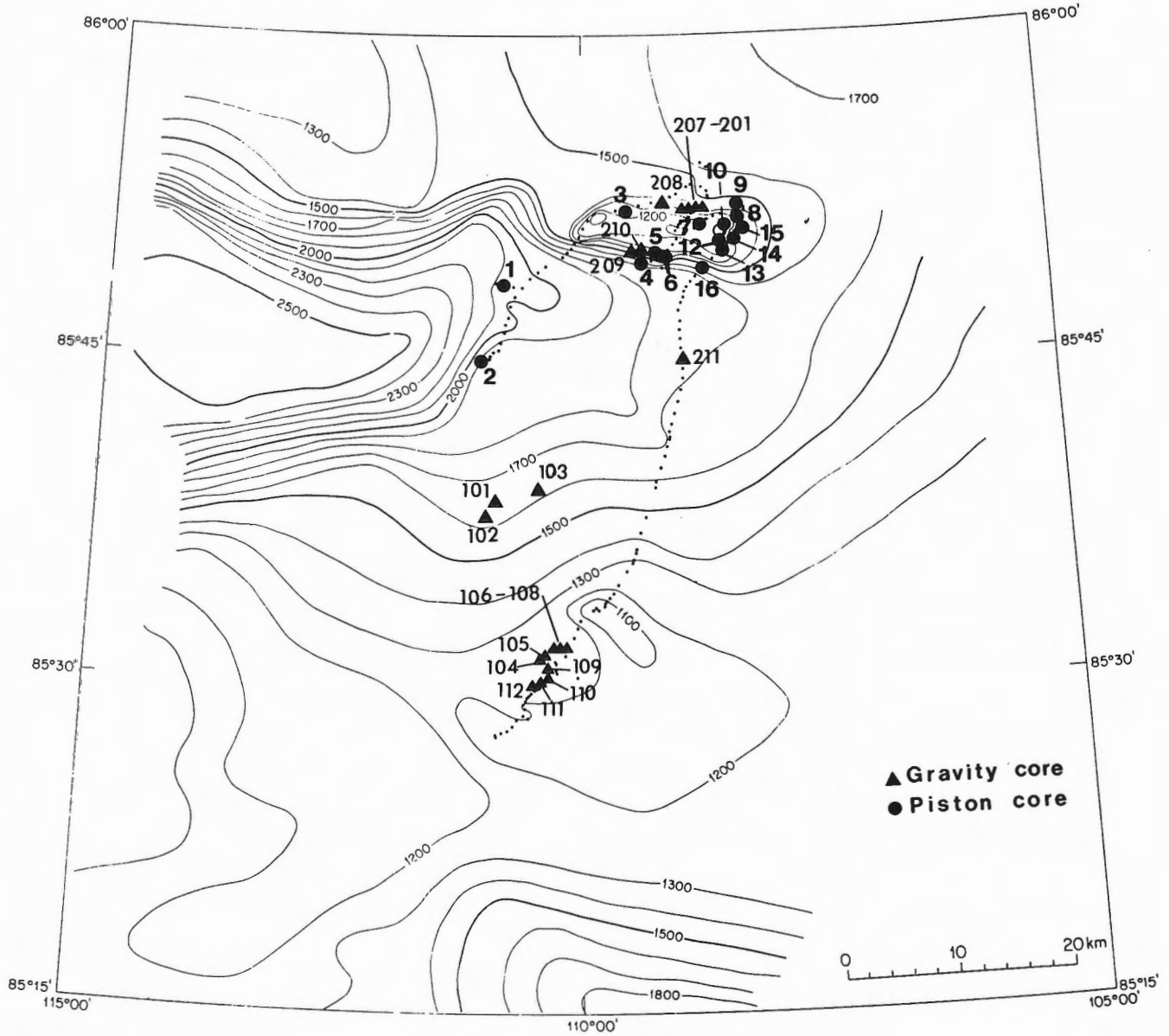

Figure 6.1 Bathymetric map of the eastern Alpha Ridge and locations of the core sites; fine dotted line is the drift track of the CESAR main camp.

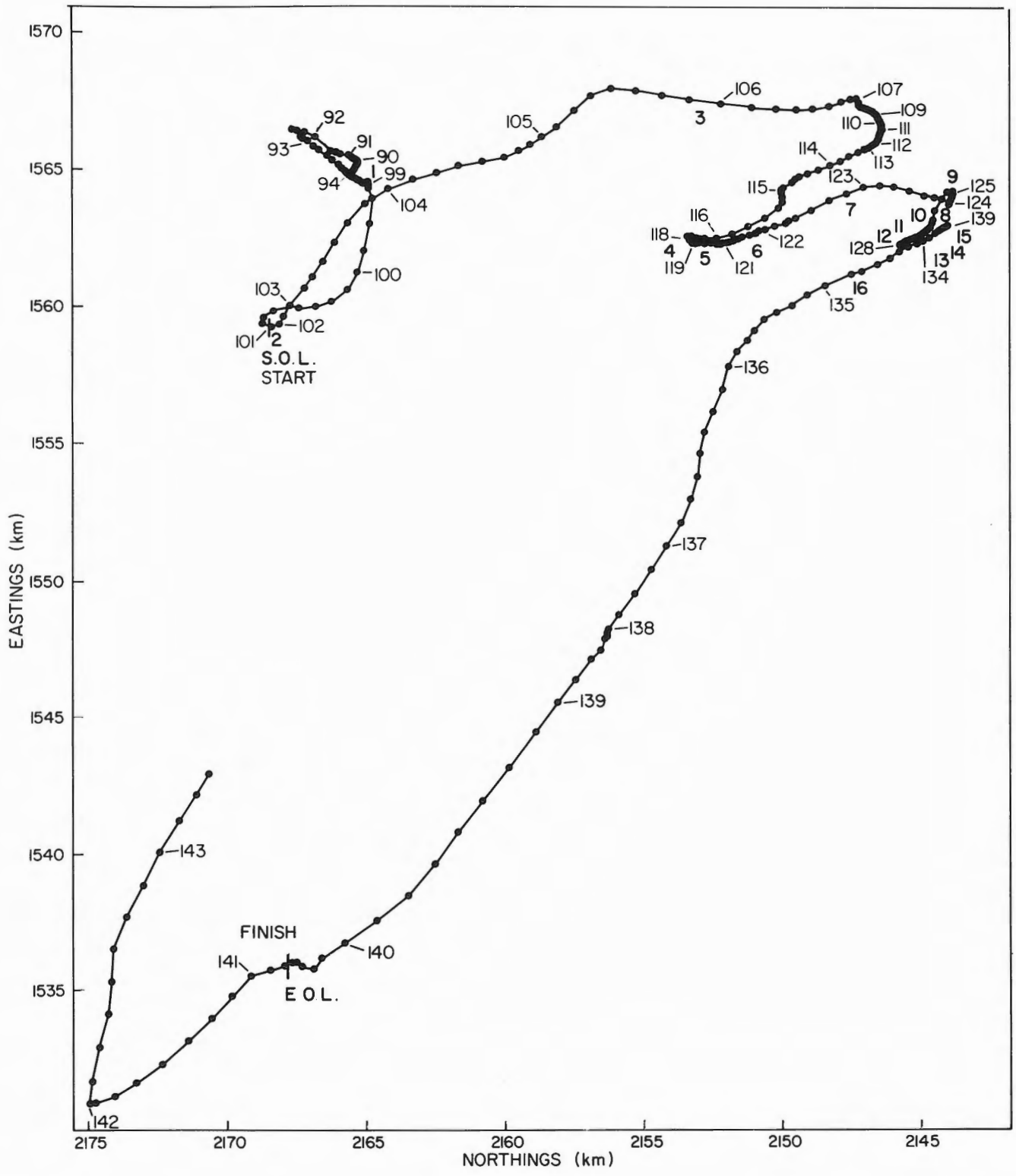

Figure 6.2 Drift track of CESAR main camp, showing time in Julian days and piston core locations (circled numbers). Vertical lines mark the start of the survey line (S.O.L.) and end of the survey line (E.O.L.).

grooves were carefully cut through with a metal blade, then the sediment was split in half by drawing nylon line down the grooves. Immediately after separation of the two core halves, sediment surfaces were covered by thin transparent plastic wrap. One core half was designated as the archive core and this was immediately enclosed in heavy plastic tubing, labelled, and stored in sealed, labelled D-tubes on horizontal racks in the refrigerated room. Wherever possible during the examination and subsequent sampling of the working core halves, care was taken to leave the thin plastic wrapping over the core surface. When not in use, the working halves were stored in the refrigerator in plastic tubing and D-tubes, as described above for the archive cores.

Figure 6.3 shows the total length of the CESAR piston cores and their composite section lengths as recovered in the field. By the time of core splitting and description, however, many of the sediment sections were slightly shorter (ca. 1-4cm) due to dewatering and settling. According to AGC core description procedures (Mudie et al., 1984), the core lengths were measured and logged in the laboratory by setting the top of the sediment in section 1 as 0cm and by assuming continuity between the sediment at the base of each section and the sediment surface at the top of the adjoining section (i.e. disregarding the presence of small empty sections at the tops of some core liners). This procedure should be carefully noted by all persons who wish to re-examine or sample the CESAR cores. It should also be noted that the field numbering system, which logged the cores as CESAR 83-001 to CESAR 83-211 was systematically changed in the laboratory to the shorter format of CESAR 1 to CESAR 211.

Because of the irreplaceable value of the CESAR cores and the need to carry out detailed multidisciplinary chronostratigraphic, sedimentological, biostratigraphic and geochemical studies on sediments with very slow deposition rates (average ca. 1mm per 1000 years according to studies of USGS ice island cores by Clark et al., 1980), a systematic sampling routine had to be carefully determined. This system (Fig. 6.4) was designed to ensure that the sediments were not disturbed or contaminated by sampling tools prior to high resolution paleomagnetism studies (*see* Aksu, 1985), or for CESAR 6, prior to geochemical studies of the laminated sediments.

CENOZOIC SEDIMENTS

Introduction

All except one of the CESAR cores, viz. CESAR 6, contained soft brown muds similar to those described by Clark et al. (1980) and by Herman (1974). Although the precise maximum age and paleoenvironmental interpretation of these sediments is presently uncertain (compare Herman, 1983, and Clark, 1982), there is unanimous agreement that these sediments are of late Cenozoic age. Clark et al. (1980) have also demonstrated that there is a strongly correlatable down-core sequence of 13 sediment units present in about 500 USGS cores collected over a 400,000km^2 area of the Canada Basin, including the southern crest of Alpha Ridge. For the sake of inter-regional comparison between CESAR cores and those from other parts of the Canada Basin, we adopted the following procedures for describing the CESAR cores:

1. David L. Clark (U. Wisconsin) visually examined all the CESAR cores when they were split and he delimited those lithofacies which probably correspond to the thirteen units, A-M, in the USGS cores described by Clark et al. (1980).

2. In this report, we have tried to use Clark's sedimentological criteria and nomenclature for the lithostratigraphic summaries, although our preliminary studies suggest that some of Clark's units should be redefined to better reflect mesoscale sedimentary structures and to clarify the definition of boundaries between lithofacies.

Since Clark's visit in June 1983, a more detailed description of 48 USGS cores from the eastern Alpha Ridge has been published (Minicucci and Clark, 1983), which defines several new lithostratigraphic units in order to facilitate correlation between these cores and those obtained earlier from the Chukchi Rise and western Alpha Ridge. Lithological units in four CESAR cores which have been sampled at 1-2cm intervals for magnetostratigraphic, lithostratigraphic, and biostratigraphic studies, appear to correspond more closely to Minicucci and Clark's (1983) redefined lithofacies. The details of the lithofacies in these 4 CESAR cores are described in the following section, but much more study is required before the lithofacies in all the CESAR cores can be defined and correlated precisely. Therefore, the summary diagram and descriptions in this report will mainly continue to use the generalized lithostratigraphic system of Clark et al. (1980).

Piston cores CESAR 14 and 15

These two piston cores were selected for detailed study because they appeared to contain the least disturbed and most complete lithological sequences. Both cores were obtained from a relatively small (ca. 5km wide), gently sloping basin or terrace extending from 1345-1425m on the northeastern margin of Alpha Ridge. Seismic profiles at these sites (*see* Jackson, 1985) show that subsurface reflectors are flat-lying.

Figures 6.5 and Plate 6.1 show the detailed structures and salient lithological features of CESAR 14 and 15 as determined from visual inspection, X-radiographs and initial sedimentological studies. Eleven lithological units (M to A-B) can be discerned, which correspond fairly closely to those described by Minicucci and Clark (1983); however, two or three additional units (A1-A3) are present at the base of the CESAR cores; paleomagnetic data (*see* Aksu, 1985) indicate that these units are up to 0.5 Ma older than the AB unit (ca. 3.7 Ma) at the base of the USGS cores from eastern Alpha Ridge (Minicucci and Clark, 1983).

Unit M in CESAR 14 (Fig. 6.5) is a foraminifera-rich sandy mud with a distinctive coarse yellowish (10 YR 5/4) carbonate bed at the base. This carbonate layer corresponds to the pink-white layer, PW2, of unit M and M′ (in USGS cores), but the overlying soupy mud in CESAR 14 was highly disturbed during coring, and the typical uppermost pink-

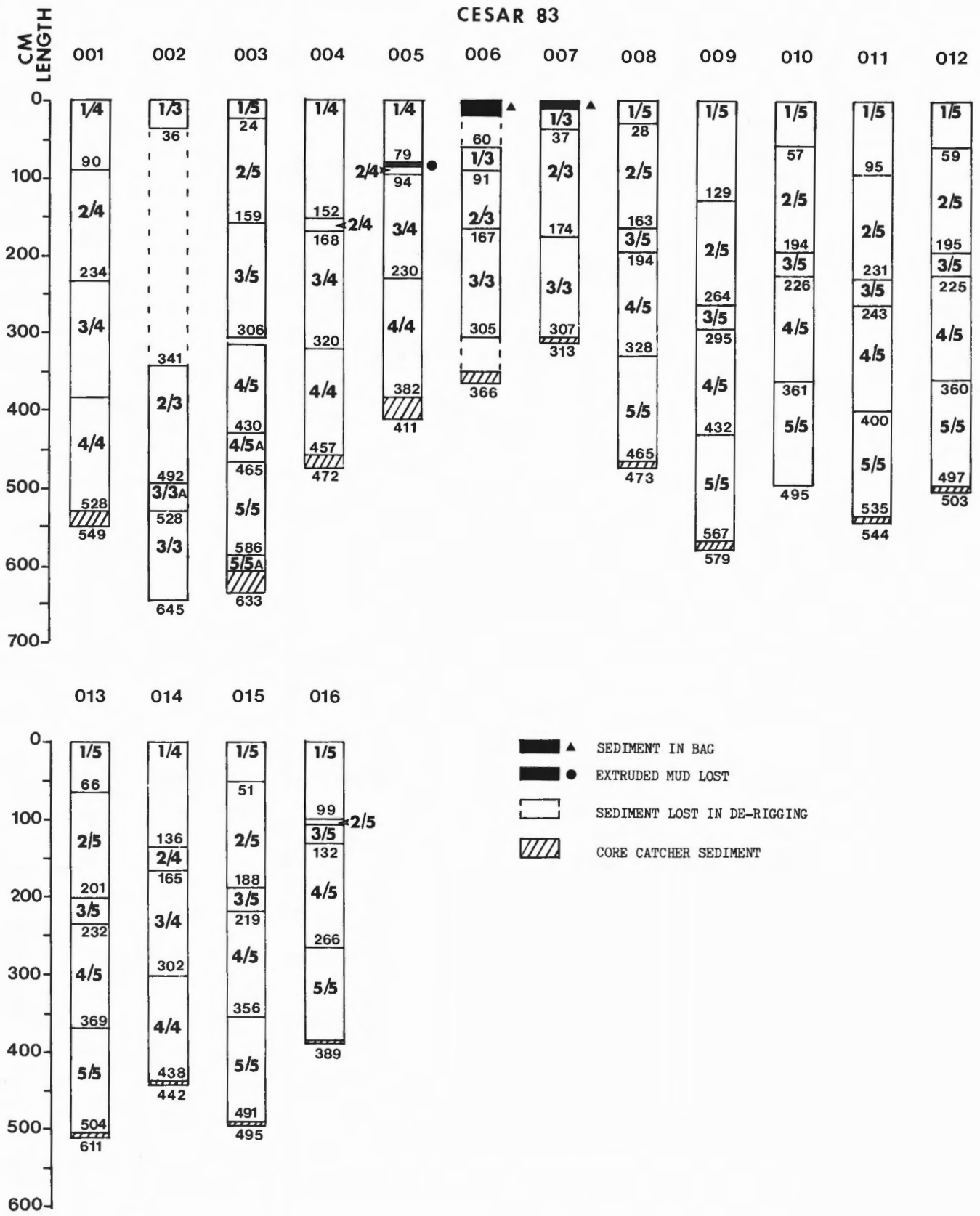

Figure 6.3 CESAR piston cores: liner section numbers (shown as fractions) and sediment lengths recovered (in cm) as recorded in the field.

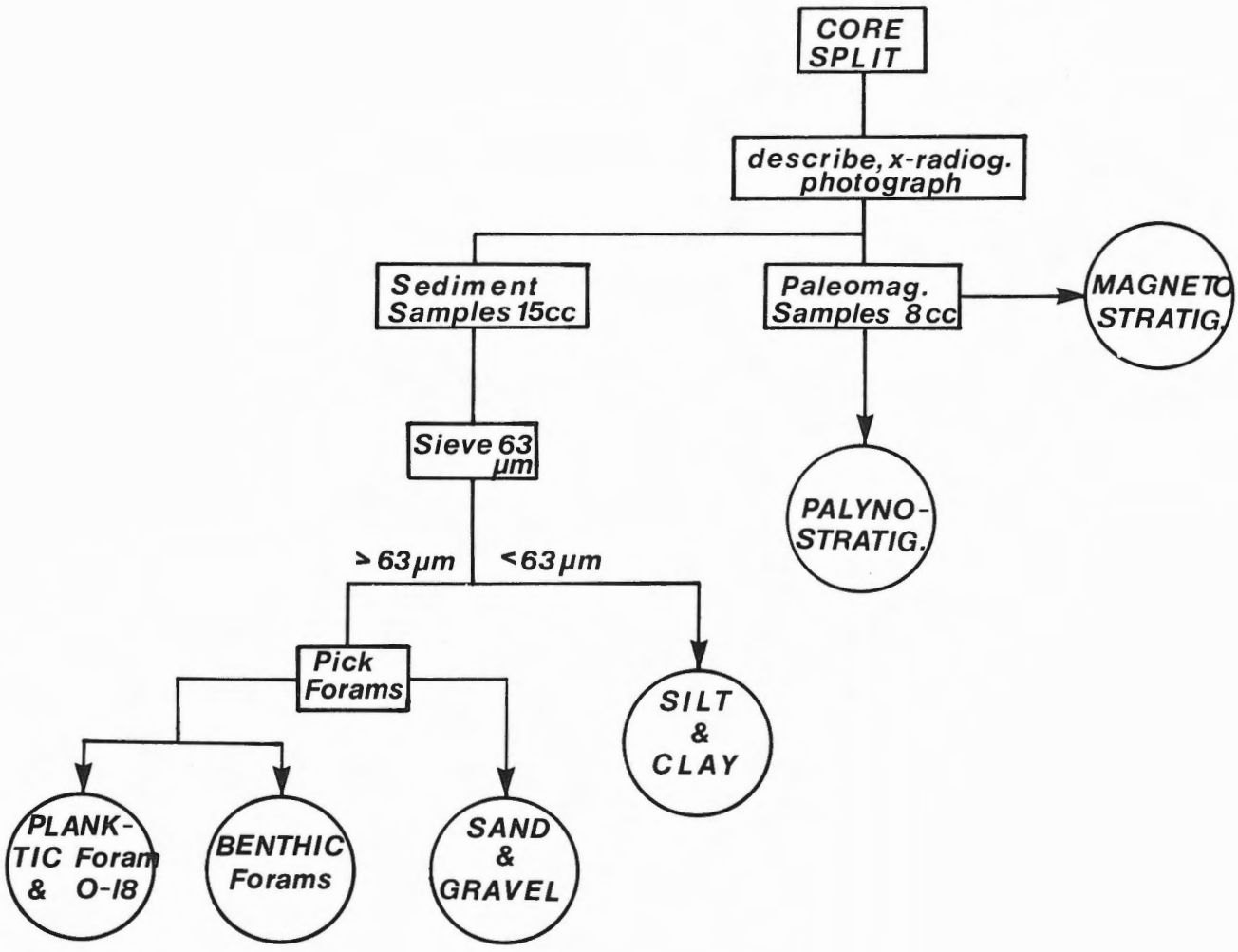

Figure 6.4 Flow chart for sampling and study of CESAR cores.

white layers, W2 and W3, appear only as scattered pebble- to gravel-sized pinkish-brown (10 YR 7/4) clasts. These upper carbonate layers and intervening sandy or silty mud beds may be more clearly seen, however, in CESAR 15 (Plate 6.1) and in several CESAR gravity cores, e.g. CESAR 103 (Fig. 6.6).

Unit L is a distinctive light olive-brown (2.5 YR 5/4), fine sandy mud, which has a darker, slightly mottled silty mud at the top. These features are typical of all the USGS cores. CESAR 14 and other CESAR cores with a well developed unit L, however, show a coarser, greyish sandy base grading upwards to finer sandy silt with 2-4 distinctive thin (2-4mm) grey sand laminae at 5-10cm intervals. Scattered grey or pinkish carbonate clasts may be present in the upper mottled layer.

Unit K is a dark brown (10 YR 3/3) silty to sandy mud which is heavily mottled at the base and top, and grades in the centre to a sandy bed mottled with grey or pale brown carbonate-rich clasts. This carbonate layer appears to correspond to W1 of Minicucci and Clark (1983) but their other subunits K′1 and K′2 cannot be discerned in the CESAR cores.

Unit J is a pale pinkish brown (10 YR 6/3) carbonate-rich sandy to silty mud with gradational contacts at the top and base. The coarse pinkish sediment generally corresponds to the PW1 layer in the USGS cores (Clark et al., 1980; Minicucci and Clark, 1983) but no overlying white zone appears in the CESAR cores. Instead, there is a wispy, thin (4mm) basal pinkish lamina in CESAR 14, which is overlain by a mottled brown mud layer, then a less mottled greyish mud with a distinctive thin (0.5cm) grey sand lamina, above which is a firm pinkish carbonate layer ca. 4cm thick. A similar sequence is found in CESAR 15, but in other cores, e.g. CESAR 103, the upper carbonate layer is mixed with dark brown mud.

Unit I is a faintly banded brown silty to sandy mud which is gravelly at the base and becomes finer grained towards the top. The banding consists of layers (ca. 5-10cm thick) of heavily mottled dark brown mud that alternate with lighter brown, sparsely mottled sandy mud containing thin (3-5cm) grey sandy laminae. Unit I in CESAR 14 and 15 differs from unit I of Clark et al. (1980) in having a mottled base and gradational contact with unit H, but the charac-

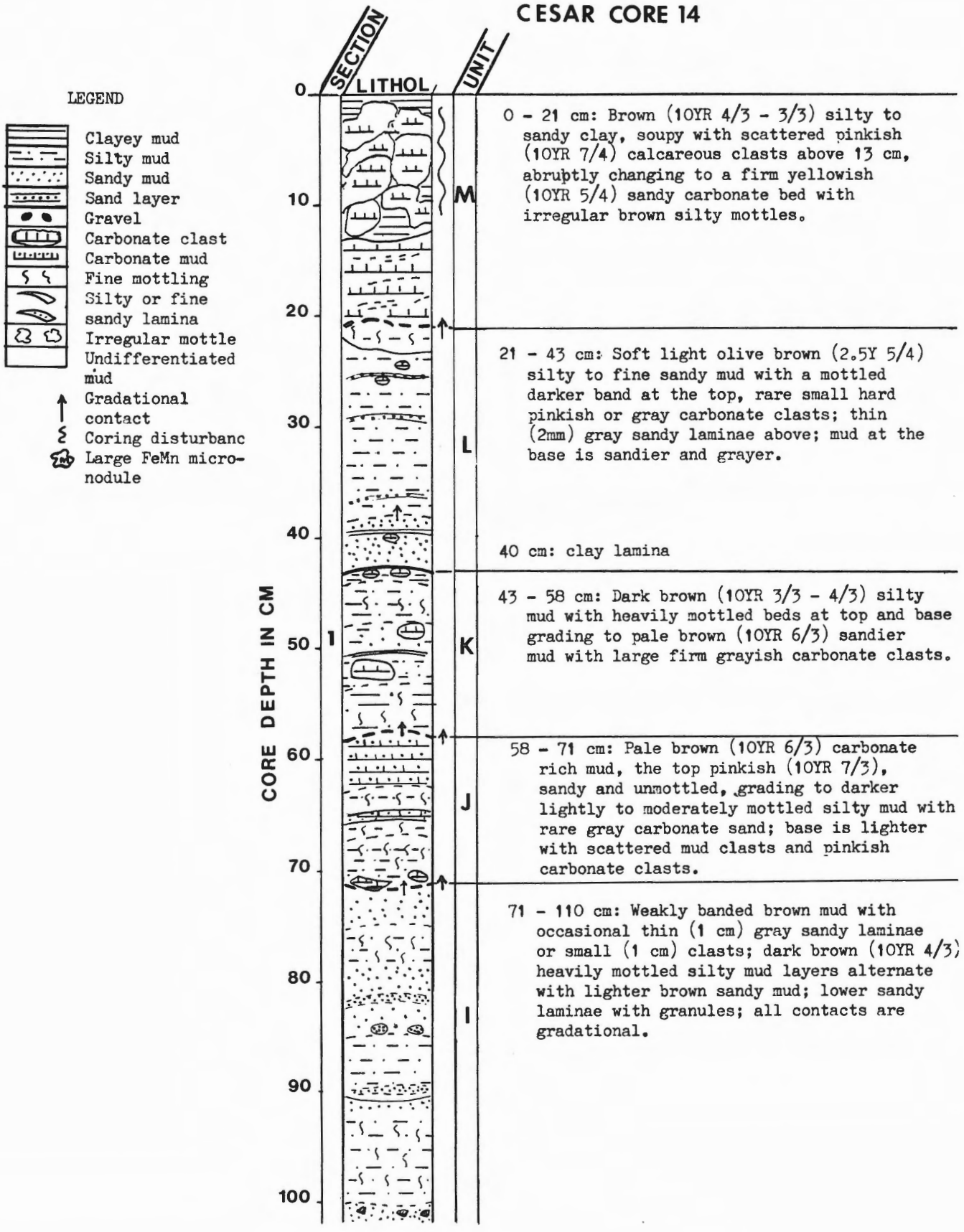

Figure 6.5 Lithological log of sediment types and structures in CESAR 14 and summary descriptions of the lithological units.

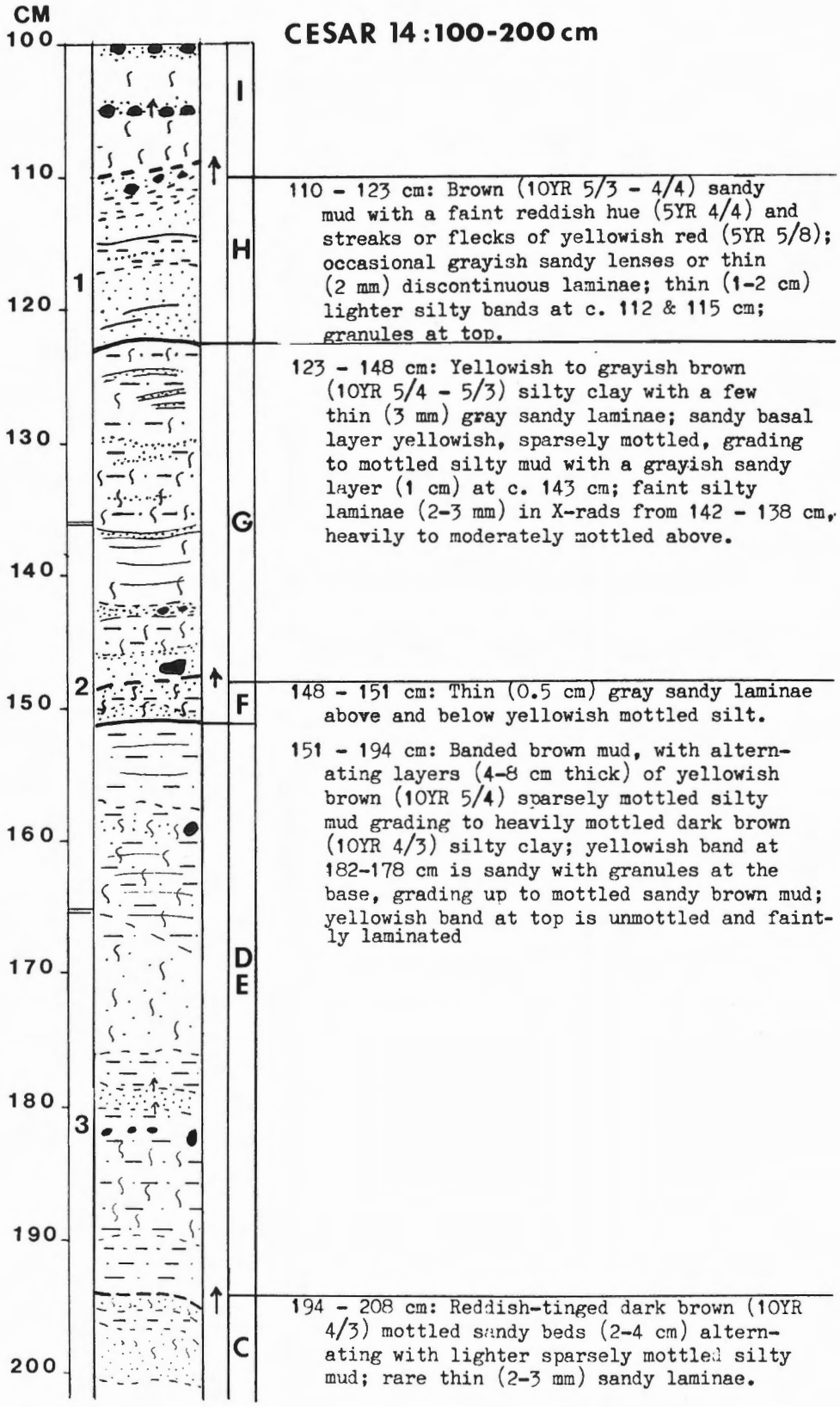

Figure 6.5 (cont'd)

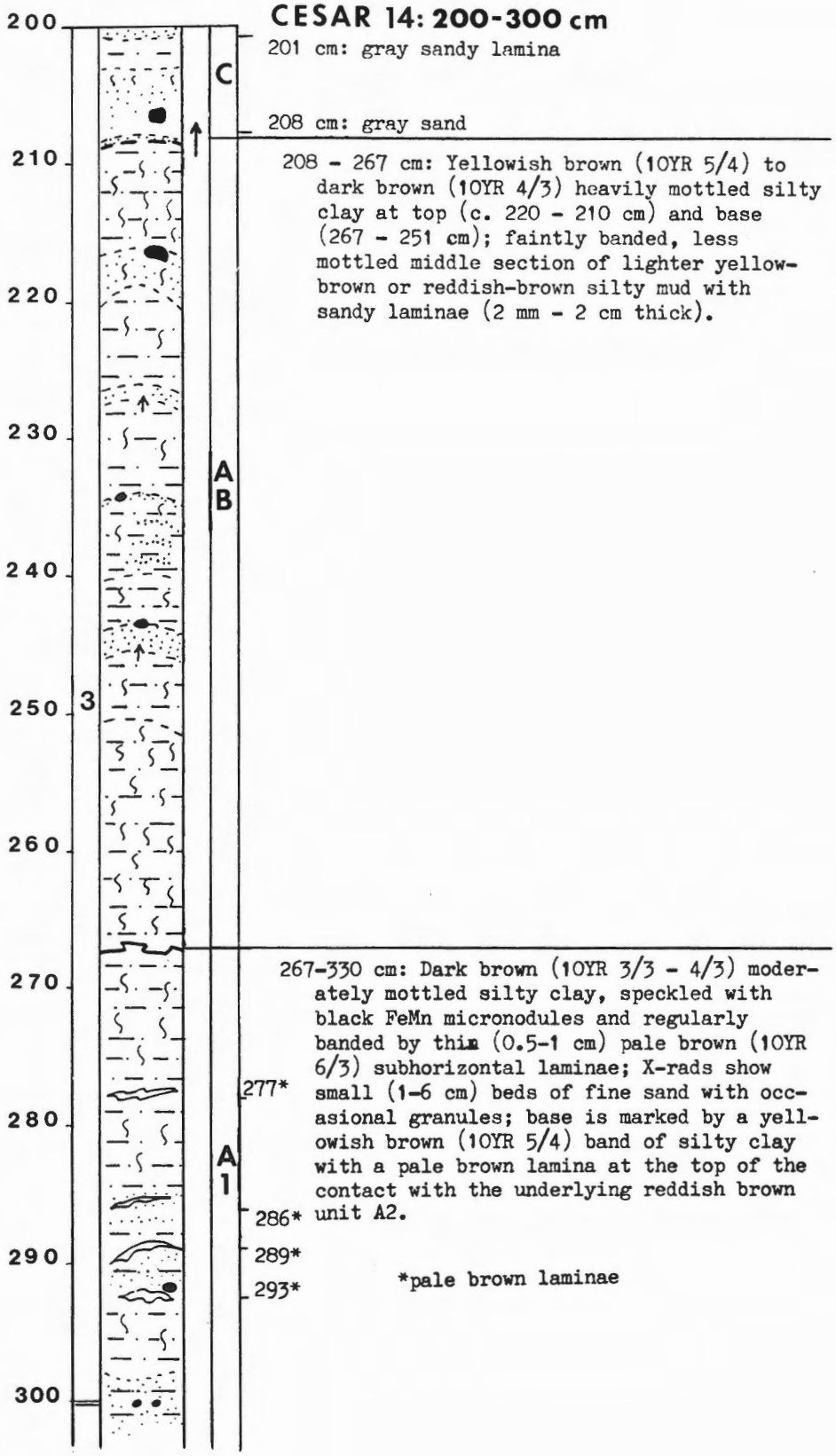

Figure 6.5 (cont'd)

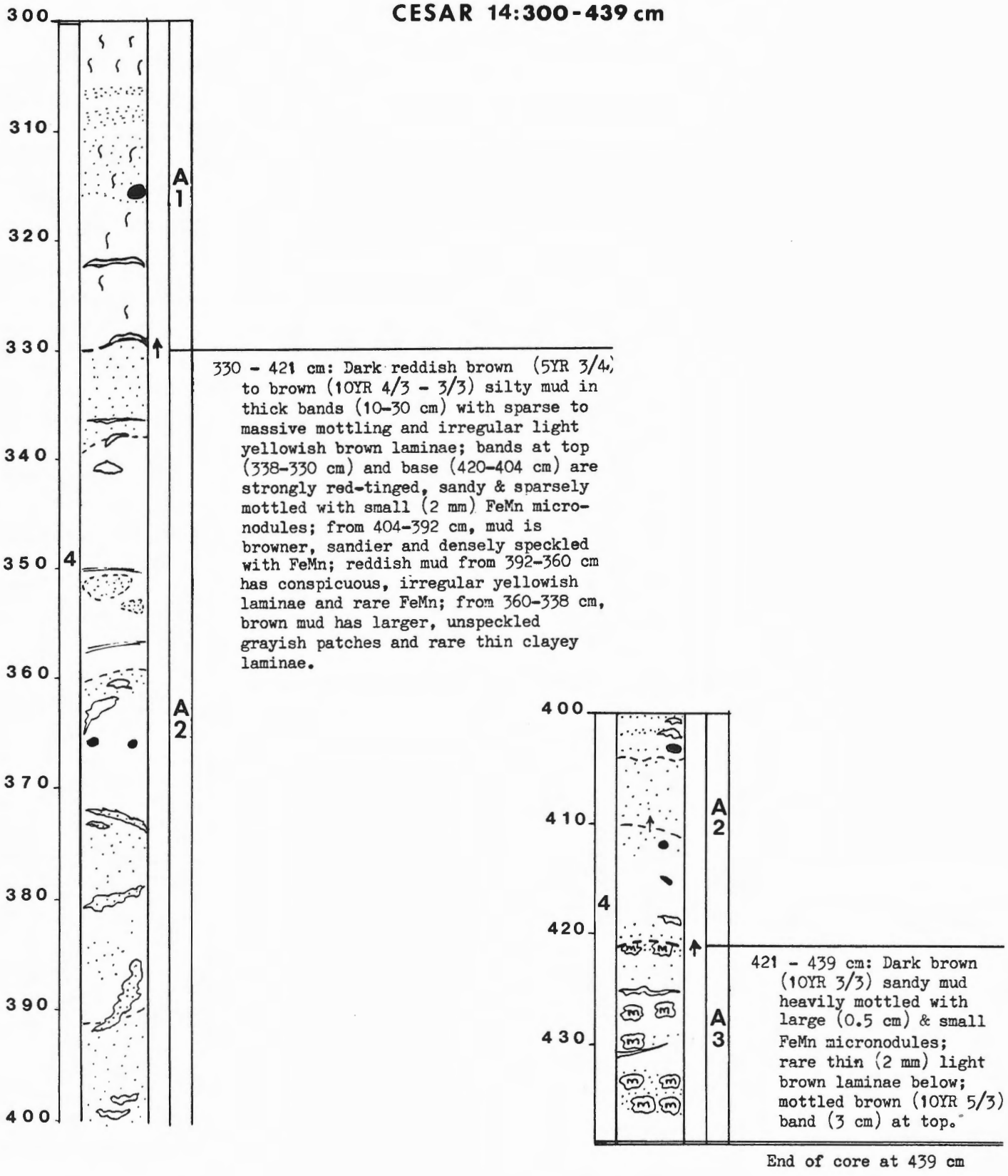

Figure 6.5 (cont'd)

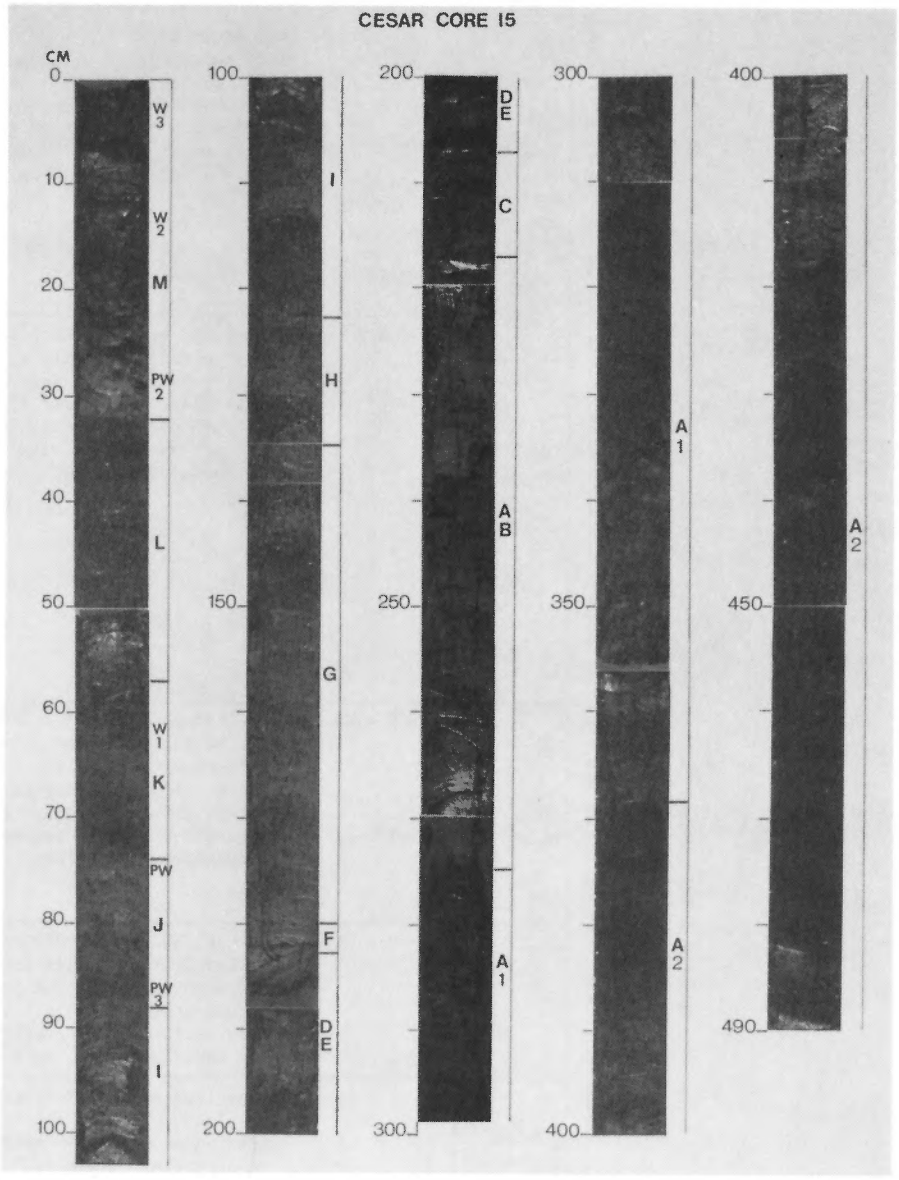

Plate 6.1

Photographic log of sediments in CESAR 15, showing the distribution of lithological units M to A2, and the position of the PW and W marker beds.

teristic central lighter brown, less mottled, sandy zone with thin grey sand laminae is present. Subunits I'1 and I'2 of Minicucci and Clark (1983) cannot be discerned in the CESAR cores.

Unit H in CESAR 14 and 15 is a reddish-tinged brown sandy mud, with a central layer (ca. 2-3cm) of lighter, less mottled silty mud. It is also characterized by the presence of three thin (4mm) grey sand laminae spaced 2-4cm apart. The basal contact is fairly sharp but the top is heavily mottled and grades into unit I. Subunits Ha through He of Clark et al., (1980) cannot be distinguished in CESAR 14 and 15.

Unit G is a moderately to lightly mottled yellowish to greyish brown silty mud with several thin (3mm) grey sandy laminae. The basal half is generally lighter coloured than the top and the basal contact is gradational, making it difficult to distinguish from unit F in all the CESAR cores. Unit F is characterized by two thin (1cm) mottled dark brown layers containing grey sand laminae and separated by lighter brown, sparsely mottled silty mud. A sandy grey lamina at the base of unit F forms a sharp contact overlying the light brown mud at the top of unit D-E; the top of the unit is gradational. In general, unit F in the CESAR cores does not closely match either unit F of Clark et al. (1980) or F' of Minicucci and Clark (1983).

Unit D-E is a banded brown mud with a yellowish, sparsely mottled silty layer (5-10cm) at the top and base, and a yellowish central band of sandy to gravelly mud. Other darker brown, mottled layers with gradational contacts are also present. Unit E of Clark et al. (1980) cannot be distinguished in the CESAR cores; however, unit D-E in CESAR 14 and 15 seems similar to unit DE in the USGS cores from eastern Alpha Ridge (Minicucci and Clark, 1983).

Unit C consists of two or three reddish-tinged dark brown (10 YR 4/3) mottled sandy layers (ca. 2-4cm) which

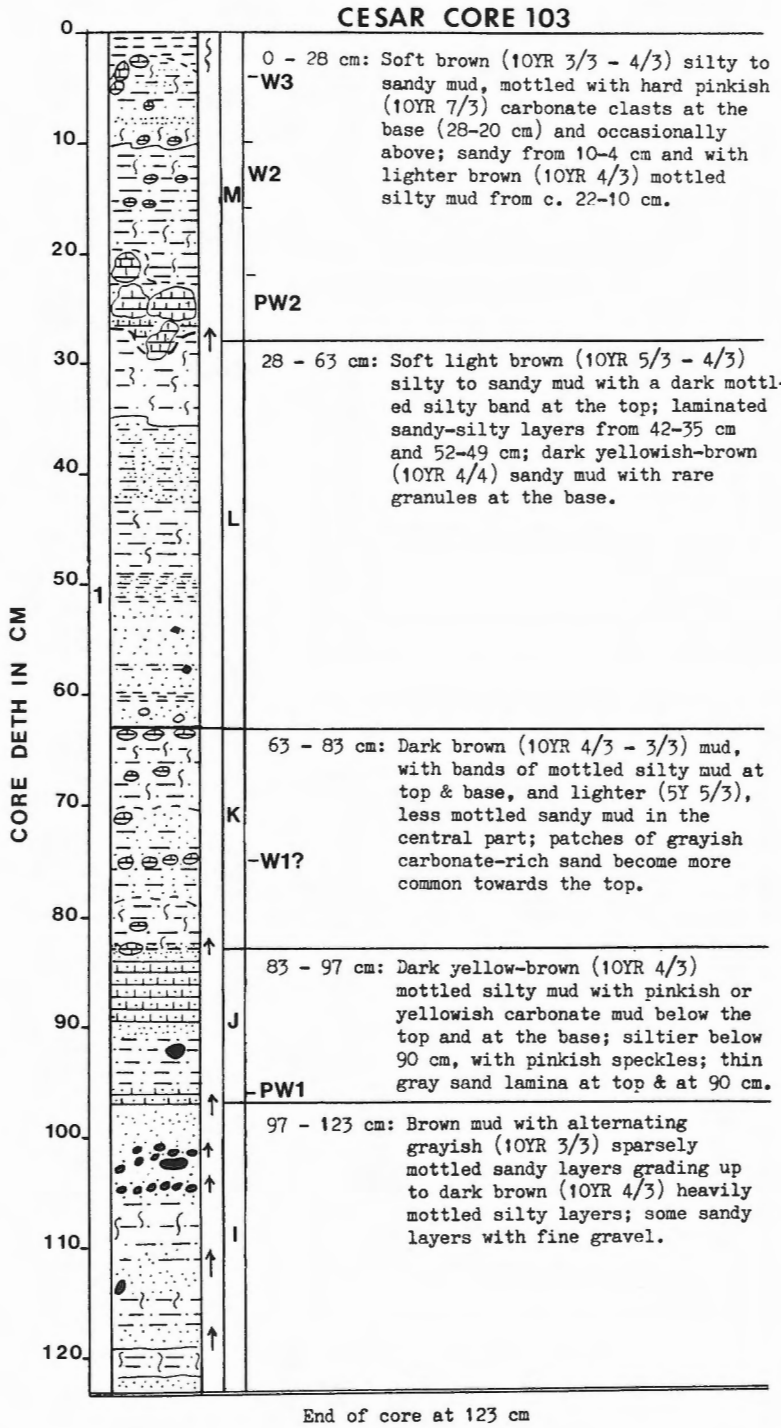

Figure 6.6 Lithological log of sediment types and structures in CESAR 103 and summary descriptions of the lithological units. See Figure 6.5 for legend to symbols used to illustrate sedimentological features.

are separated by lighter brown sparsely mottled silty mud. A thin grey sand lamina marks the base of the unit, but other contacts are gradational. This unit is only 10-20cm thick in CESAR 14 and 15, and it is not clearly distinguishable from sandy sections of unit D-E in some CESAR cores.

Unit A-B is an irregularly banded brown mud, speckled throughout with small black FeMn micronodules. From the base up, the bands consist of alternating yellowish (10 YR 5/4) mottled silty clay which grades upwards to a moderately mottled dark brown (10 YR 4/3) mud, often with sand and rare gravel at the top of the dark bands. The middle section of the unit is a lighter coloured, less mottled silty mud with thin sandy laminae. In CESAR 14 and 15, this unit appears to be similar to unit AB of the USGS eastern Alpha Ridge cores (Minicucci and Clark, 1983). In some CESAR cores, however, unit A-B is not clearly distinguishable from unit D-E.

Unit A1 is a dark brown (10 YR 3/3-4/3), moderately mottled, silty clay which is prominently marked by wispy, pale brown (10 YR 6/3), subhorizontal laminae, about 3mm to 1cm thick. The dark brown mud is regularly speckled by abundant small black FeMn micronodules. The unit contains occasional gravel, greyish mud clasts, and sandy layers or thin sand laminae. The top of the unit is marked by a sharp transition from the yellowish-brown silty mud at the base of A-B to the top of a massive dark brown mud unit with thin yellowish laminae at intervals of ca. 5-20cm. The basal contact is marked by a yellowish-brown subhorizontal lamina at the top of ca. 20cm of dark brown mud with coarse yellow mottling.

Unit A2 is a massive dark reddish-brown (5 YR 3/4) silty to sandy mud which is less speckled by FeMn micronodules than unit A1 and is conspicuously marked by blotchy or oblique-angled light yellowish-brown (10 YR 6/3) structures which resemble burrows ca. 1cm thick. The lower half of the unit and the top 10cm are sandy; the middle section is more silty, less speckled by FeMn, and includes greyish sandy layers 2-10cm thick in CESAR 14. The base of the unit is marked by a conspicuous increase in relatively large (ca. 0.5cm) FeMn micronodules at the top of unit A3.

Unit A3 is a very dark brown (10 YR 3/3), slightly sandy mud which is conspicuously mottled by relatively large (0.5cm) black FeMn micronodules in addition to abundant small black FeMn speckles. Irregular bands (2cm) or small blotches of speckled light brown mud are occasionally present. The top of unit A3 is marked by a subhorizontal band of greyish dark brown mud with large black FeMn micronodules at the base of the massive dark reddish-brown mud of unit A2.

Gravity cores CESAR 102 and 103

These two cores were selected for detailed study because they contain the longest sequences of sediment recovered by the gravity corer. Both cores were obtained from gently sloping areas on the southeast side of the Alpha Ridge graben, at depths of ca. 1500m or more. Only shallow seismic data (3.5 kHz) are available for these sites, but a similar stratigraphy was obtained in CESAR 201 from the edge of a basin on the north side of the northern Alpha Ridge crest (Fig. 6.1). The seismic profile for this area (*see* Jackson, 1985) shows smooth, flat-lying surface reflectors at this site, compared to neighbouring sites of CESAR cores 202 and 203 where surface reflectors appear truncated, and shorter gravity cores were obtained.

Figure 6.6 shows the detailed structures and salient lithological features of CESAR 103, the longest gravity core; Figure 6.7 depicts the lithofacies and marker beds in CESAR 102, 103 and all other gravity cores containing more than 5cm of sediment. The magnetochronology, foraminiferal biostratigraphy, and palynostratigraphy of CESAR cores 102 and 103 are described by Aksu (1985a,b) and Mudie (1985) respectively. The main lithostratigraphic characteristics of the gravity cores are outlined as follows.

Unit M in core 103 consists of ca. 28cm of dark brown (10 YR 3/3) soft mud which is variably mottled or banded by pinkish (2.5 YR 6/4) to yellowish-brown (10 YR 7/3) carbonate-rich "hardground" layers. At the surface (0.2cm) there is a soupy, foram-rich, dark brown mud layer which coarsens downwards to mud with scattered carbonate hardgrounds and much lower foram concentrations. This carbonate layer probably corresponds to the W3 subunit of the USGS cores (Minicucci and Clark, 1983). From ca. 4-9cm, there is a greyish (5 YR 5/3) sandy mud layer with dark mottles and low foram concentrations. From 9-ca. 22cm, there is a layer of heavily mottled, foram-rich, dark brown (10 YR 3/3) silty mud with scattered small (<1cm) pinkish hardgrounds. These pinkish clasts are most conspicuous in the middle of this dark layer and may correspond to the W2 subunit of the USGS cores; in general, however, there is no distinctive whitish W2 carbonate layer in the CESAR cores. At ca. 22cm in CESAR 103, the dark brown mud is interlayered with large pinkish (10 YR 7/3) semiconsolidated carbonate-rich clasts which increase in size towards the base at ca. 28cm. This layer clearly corresponds to the PW2 subunit of the USGS cores. It also corresponds to an interval over which foram concentrations decrease greatly.

Similar lithological sequences are easily recognised in unit M of CESAR 102, 201, and 210, all of which are from water depths of ca. 1500m or more. In these cores, unit M varies in thickness from 41cm in CESAR 210 to 37cm in CESAR 102. The main differences among the cores appear to be in the thickness (10-20cm) of the mottled brown mud containing the ?W2 layer; however, the sandy mud is also thicker (10cm) in CESAR 210, and the PW2 layer ranges from ca. 8cm in CESAR 103 to 12cm in CESAR 102 and 210.

Unit L in CESAR 103 consists of about 35cm of light brown (10 YR 5/3-4/3) to olive (2.5 YR 5/4) silty or sandy mud which has a distinctive mottled brown band at the top and a dark brown layer with thin (ca. 2cm) greyish sandy laminae and scattered gravel below 50cm; the contact with unit M is gradual. The top of the upper mottled band contains relatively low foraminiferal concentrations which increase downwards in the mottled layers to ca. 35cm; from here to the base of the unit, however, foraminifera are rare or absent. The base of unit L in CESAR cores 103 and 102 is sharply defined by a greyish, coarse sandy layer overlying the dark brown,

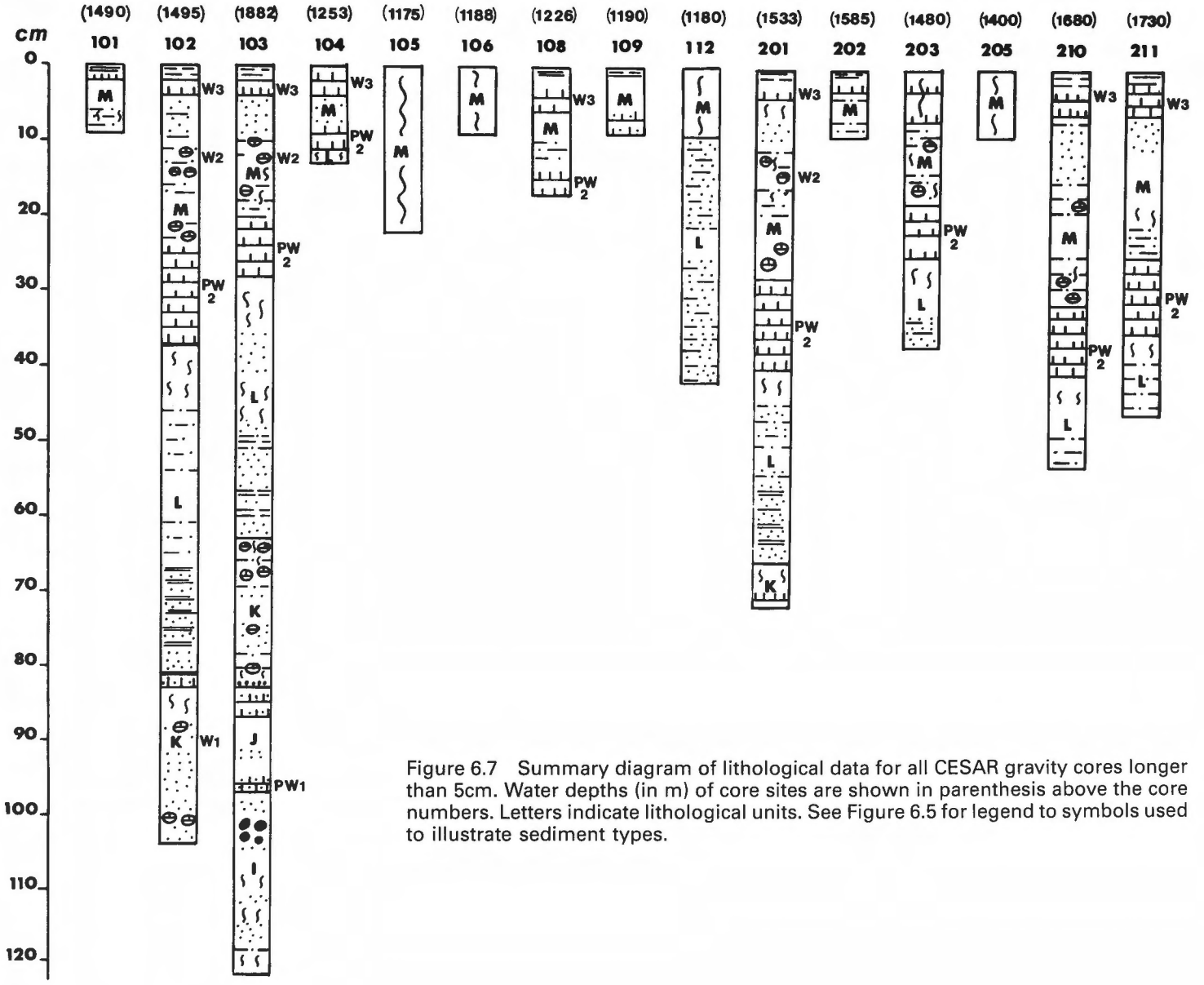

Figure 6.7 Summary diagram of lithological data for all CESAR gravity cores longer than 5cm. Water depths (in m) of core sites are shown in parenthesis above the core numbers. Letters indicate lithological units. See Figure 6.5 for legend to symbols used to illustrate sediment types.

mottled carbonate-rich mud layer at the top of unit K. From the base of unit L up to core depths of 35cm in CESAR 103 and ca. 46cm in CESAR 102, there is a fining-upward sequence of dark yellow (10 YR 4/4) sandy layers (2-6cm thick) alternating with thinner (ca. 1cm) silty layers, followed by a lighter brown slightly mottled silt layer ca. 6cm thick, then unmottled olive-brown fine sandy silt.

In the 4 gravity cores containing a complete unit L, the thickness of this unit ranges from 26-44cm; in the piston cores, the thickness of unit L ranges from 15-31cm. This difference is probably partly due to greater compaction in the piston cores, but in both piston and gravity cores, the unit appears to be thinner and less well differentiated at shallower (<1500m) sites. This feature requires further study in order to understand the depositional orgin of unit L.

Unit K in CESAR 103 consists of ca. 20cm of dark brown mud with 5-7cm of heavily mottled silt at the top and base, and a lighter brown, sandy middle section containing greyish patches and rare carbonate-rich clasts. Foraminifera are abundant in the top layer but they decrease substantially towards the base. The base of unit K is marked by a greyish sandy layer, but it is not sharply distinguished from the top of unit J. The grey carbonate-rich clasts in the centre of the unit may correspond to the W1 layer of the USGS cores, but none of the CESAR cores show the distinct whitish band described by Minicucci and Clark (1983).

Unit J in CESAR 103 consists of ca. 14cm of mottled yellow-brown sandy to silty mud with pinkish carbonate-rich mottles at the top and a distinctive thin (1cm) pinkish-yellow layer at the base. As in unit K, the top mottled layer is rich in foraminifera, but they become very sparse below the 90cm level which is marked by a thin (1cm) grey sand layer. The pinkish carbonate layer at the base corresponds to the PW1 marker in the USGS cores.

Unit I in CESAR 103 consists of 26cm of brown mud with greyish (10 YR 3/3) sandy layers 2-8cm thick which fine upwards to dark brown (10 YR 4/3) heavily mottled silty layers. Foraminifera are rare in this unit which appears to be very similar to the top of the much longer (36-80cm) unit I found in CESAR piston cores.

Correlation and paleoenvironmental interpretation

Figures 6.7 and 6.8 show that the lithological units in most of the CESAR gravity and piston cores can be correlated over the 3600km^2 area covered by CESAR, despite the wide range in water depth (2150-1180m) and the differences in bottom topography at the core sites. Magnetostratigraphic data for CESAR cores 14, 102 and 103 (Aksu, 1985a) indicate that the boundary between the Brunhes and Matuyama magnetochrons lies in unit K. The generally accepted age of this boundary is 0.73 Ma (Harland et al., 1982). If a constant sedimentation rate is assumed for those cores containing units M-K, it can be estimated that sedimentation rates during the past 0.73 Ma are between 0.77 and 1.2mm per Ka. These values agree well with the mean sedimentation rate of 1.17mm.$^{-1}$Ka obtained for non-turbidite Late Pleistocene deposits in the USGS cores from Alpha Ridge and Chukchi Rise (Minicucci and Clark, 1983).

In general, the top sections (units M-I) of the CESAR cores and the USGS cores from Alpha Ridge show a similar succession of bioturbated, foram-rich carbonate muds alternating with less bioturbated silty-sandy intervals containing relatively few foraminifera. Clark et al. (1980) interpret the silty muds as representing intervals of sea ice sedimentation corresponding to glacial maxima; the sandy muds, including carbonate-rich layers, are considered to represent intervals of sediment deposited by sea ice and icebergs during warmer climatic stages. Glacial-marine sediment transport is the most reasonable explanation for the very widespread occurrence of these correlatable lithologies in the Canada Basin and for the presence of coarse material of non-local origin on the Alpha Ridge during the past 1 Ma. However, further sedimentological study is required in order to provide a more definite interpretation of the factors responsible for the foram-poor carbonate hardground layers and the unproductive sandy mud facies of units L and I. Palynomorphs in unit L (Mudie, 1985) suggest increased fluvial input during this interval.

Chronostratigraphic correlation and paleoenvironmental interpretation of units H to A3 in the CESAR piston cores is presently much less certain than for the upper Pleistocene units, M-I. This is due to several factors: i) difficulty in defining the boundaries and distinguishing between the lithologies of the sandy units H, F and C which are the primary means of delineating the tops of silty mud units G, D-E and A-B; ii) in CESAR cores 2, 4-7 and 11, there are either large hiatuses due to coring disturbance or due to intervals of nondeposition in sediments above unit A-B; iii) flow-in and other coring artifacts, such as re-entry of the corer at the seabed, have disturbed the primary structures in the lowest parts of several cores. For example, pinkish carbonate clasts with abundant planktonic forams are present up to 75cm above the bases of CESAR 8, 10 and 11, in sharp contrast to typical siliciclastic mud of units A1-A3 which usually contain only thin layers of arenaceous forams.

The summary data (Table 6.2) for unit thickness in the CESAR piston cores, however, can be used in conjunction with seismic reflection data (Jackson, 1985) to draw some tentative conclusions about older Late Cenozoic sediments on Alpha Ridge.

1. The sandy-gravelly muds of units H, F and C are relatively uniform in thickness and contain coarse sediment that could only have been transported to the Alpha Ridge by ice during intervals of extensive continental glaciation. Paleomagnetic data (Aksu, 1985a) indicate that unit C approximately corresponds to the Pliocene-Pleistocene boundary (ca. 1.8 Ma).

2. The mottled brown silty mud units (G, D-E, A-B, A1 and A2) generally increase in thickness down-core and the number of clasts decreases, especially below unit D-E. This suggests that intervals of iceberg-transported glacial debris were much less frequent during the late Tertiary interval. In CESAR 14, the boundary between the Gauss and Gilbert magnetochrons (ca. 3.4 Ma) lies near the base of unit A1, and

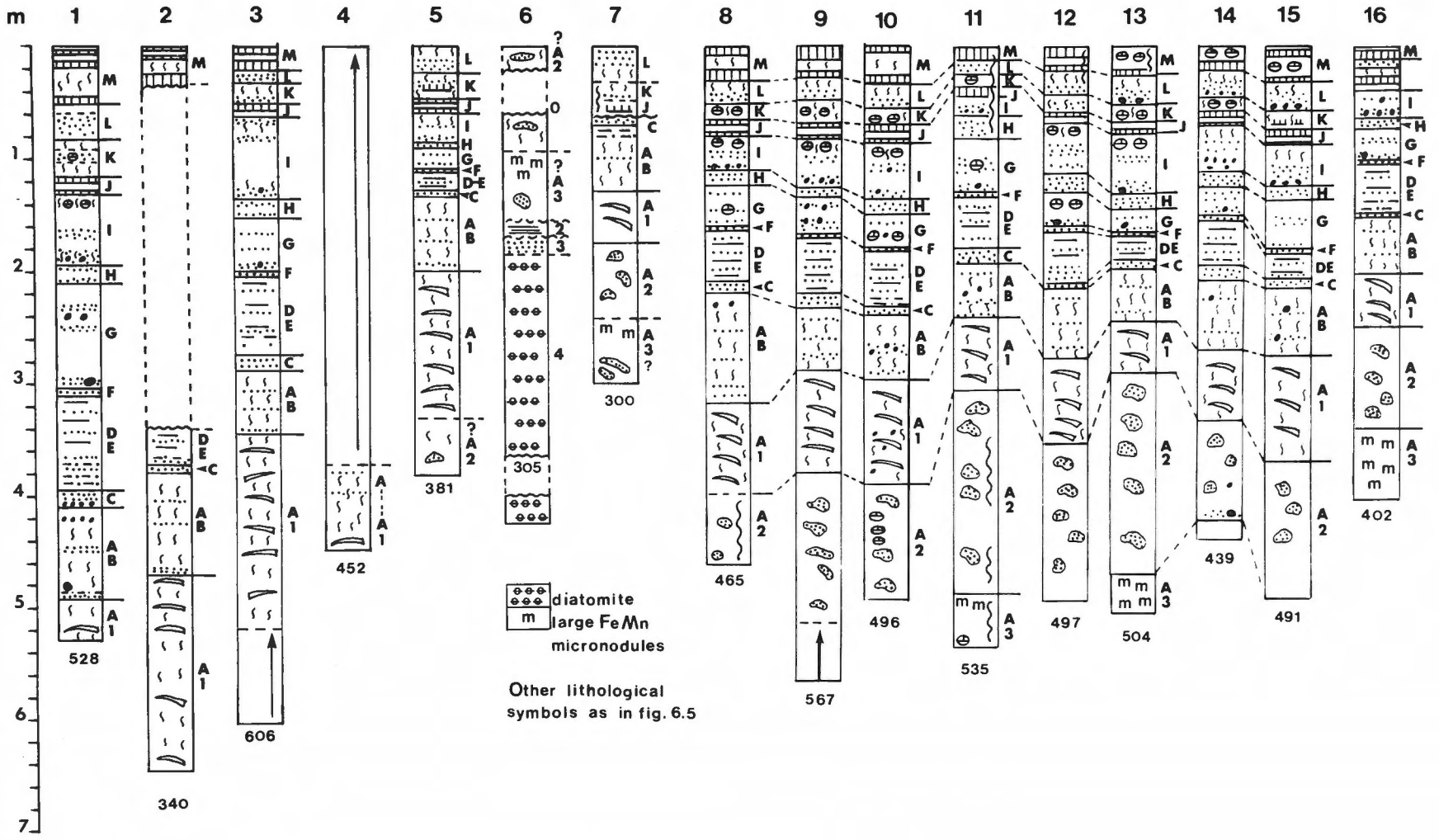

Figure 6.8 Summary diagram of lithological data for CESAR piston cores. Upper case letters indicate lithological units for late Cenozoic sediments; core lengths (in cm) as logged in the laboratory are shown for each core.

Table 6.2 Thickness of sediment units (in cm) in CESAR piston cores.

Core No.	1	2	3	4	5	6	7	8	9	10	11	12	13	14	15	16	
Water Depth (m)	2150	1900	1300	1725	1680	1365	1250	1460	1500	1425	1380	1345	1360	1370	1405	1500	Mean & (Range)
Unit M	51	30	22	ND	0	0	0	30	29	32	8	20	24	21	32	9	26 (8-51)
Unit L	31	0	15*	ND	23	0	29	21	21	21	15	21	26	22	25	10	22 (10-31)
Unit K	32	0	17	ND	24	0	23	13	17	17	10	13	16	15	17	7	17 (7-32)
Unit J	20	0	12	ND	13	0	5	9	15	18	9	11	12	13	14	14	13 (9-20)
Unit I	62	0	69	ND	23	0	0	38	44	47	18	47	56	39	35	24	42 (18-69)
Unit H	14	0	19	ND	5	0	0	14	9	14	21	17	11	13	12	11	13 (5-19)
Unit G	97	0	46	ND	21	0	0	37	32	30	47	30	19	25	45	26	38 (19-51)
Unit F	6	0	4	ND	3	0	0	2	5	3	4	6	3	3	4	3	4 (2-6)
Unit D-E	89	24	71	ND	18	0	8	48	47	50	47	37	23	43	23	43	45 (23-89)
Unit C	6	5	14	ND	5	0	3	8	14	8	13	12	8	14	10	3	9 (3-14)
Unit A-B	86	85	58	ND	65	0	61	100	57	59	48	62	47	59	59	51	64 (47-86)
Unit A1	34	180	429	ND	130	0	43	80	91	92	64	78	43	63	92	48	75 (43-130)
Unit A2	ND	ND	ND	ND	51	90	66	52	186	104	206	142	182	91	122	91	137 (91-182)
Unit A3	ND	ND	ND	ND	ND	70	58	ND	ND	ND	25	0	34	18	0	62	45

*part missing

the base of this core has an a estimated age of ca. 4.5 Ma. Palynological data from unit A3 in CESAR 14 (Mudie, 1985) also indicate a Late Miocene to Early Pliocene age for the base of this core.

3. Several of the lithofacies below unit F contain beds of graded sediment ca. 10-20cm thick. The relatively uniform thickness of the units in cores from different topographic settings, however, combined with the ubiquitous presence of bioturbation and apparently authigenic ferromanganese micronodules, indicates that the thick pre-Pleistocene brown mud units are not gravity flow deposits but were laid down slowly in an oxidizing sedimentary environment.

4. Units A2 and A3 contain thin beds of well preserved deep-water arenaceous foraminifera which alternate with layers of corroded planktonic forams and poorly preserved arenaceous foraminifera. This suggests that the southeastern Alpha Ridge was not continuously covered by ice during the Pliocene but that cyclical paleoceanographic changes regulated the productivity and/or preservation of biogenic material. Palynological data (Mudie, 1985) suggest some aeolian transport of fine sediment from regions of subartic vegation, but there is little evidence for increased fluvial sediment transport to the Alpha Ridge during the early Pliocene.

5. Despite the relatively shallow water depth (1500m) of most of the CESAR piston cores, there is a remarkable change from intervals of carbonate-rich sediments in the Pleistocene-Recent sediments to Late Tertiary siliciclastic sediments in which both calcareous and siliceous microfossils are rare and poorly preserved. Herman (1983) considers that these unfossiliferous sediments reflect productive subarctic waters with a very shallow lysocline which inhibited preservation of calcareous microfossils, as presently found in Baffin Bay (Aksu, 1983). Holocene sediments in Baffin Bay, however, are very rich in diatoms and dinoflagellates (Mudie and Aksu, 1984), whereas the Alpha Ridge sediments are relatively unproductive. This difference can probably be explained by: i) a much slower sediment accumulation rate in the Arctic Ocean (2mm.Ka^{-1} compared to 20mm.Ka^{-1} in Baffin Bay); and ii) lower influx of humic organic material to the Alpha Ridge area. Slow sedimentation would mean long exposure to oxidizing silica-depleted bottom water, hence the dissolution of thin-walled planktonic siliceous microfossils and the oxidation of organic matter, including palynomorphs. Low influx of humic acids due to infrequent transport of terrigenous debris by ice or meltwater would also suppress dinoflagellate productivity. Future studies of sand grain surfaces, clay mineralogy and the provenance of clasts in the Tertiary lithofacies are required, however, before the existence of an extensive ice-cover (Clark, 1982) can be dismissed as a possible cause of the unproductive Early Pliocene muds in the Artic Ocean.

CRETACEOUS LAMINATED SEDIMENT

Introduction

CESAR 6 (Plate 2) was recovered from a water depth of 1365m on the south side of the northern crest of Alpha Ridge, at latitude 85°49.8′N, longitude 109°09.2′W. Shallow seismic reflection profiles near this site (Fig. 6.9) show that the core site is located on a fault block where a prominent subsurface reflector lies very close to the seabed. West of the core site, a fault line appears to mark the edge of the Alpha Ridge graben, and chaotic reflectors suggest the accumulation of massive slump-block and debris-flow sediments on the side of the trough below the site of CESAR 6.

Figure 6.10 illustrates the salient lithological characteristics and sediment structures in CESAR 6. The core catcher recovered about 12cm of very soft, olive-grey to yellow-brown siliceous mud, containing common unweathered quartz sand and thin, bubble-wall, glassy volcanic shards. Traces of laminated structure are indicated by crumbly blocks of firm, light olive siliceous ooze containing thin (2-5mm) continuous layers of light brown mud. Silicoflagellates (Bukry, 1985), diatoms and palynomorphs (Mudie, 1985) indicate a Late Campanian to Danian age for the siliceous ooze. Bulk samples, however, contain rare specimens of very well preserved *Neogloboquadrina pachyderma* (identified by W.H. Berger and G. Keller) which has an age range of Miocene-Recent, thereby indicating that the corer probably bounced on the seabed and dragged in some surface mud prior to penetration and triggering of the piston. Some yellowish sediment also washed out from the core base on removal of the catcher (see Fig. 6.3 for reconstruction of sediments cored at Site 6).

The core liner of CESAR 6 retained 305cm of sediments, including 4 visually distinctive lithological units. Unit 1 (0-99cm) is a soft brown (10 YR 4/3) silty to clayey mud, irregularly mottled with yellowish-brown (10 YR 5/4) streaks. Occasional silt to fine sand laminae or scattered coarse sand and rare gravel are present. Small to large (0.5cm) black FeMn micronodules occur below 30cm. Microfossils are very rare and are mostly poorly preserved, including biogenic silica fragments, rare highly oxidized pollen and rare foraminifera. At present this unit cannot be dated with certainty but its appearance, mineralogy and microfossil content is very similar to units A2 and A3 of CESAR core 14, which are of Late Miocene-Early Pliocene age. Rare palynomorphs from the base of unit 1 (Mudie,

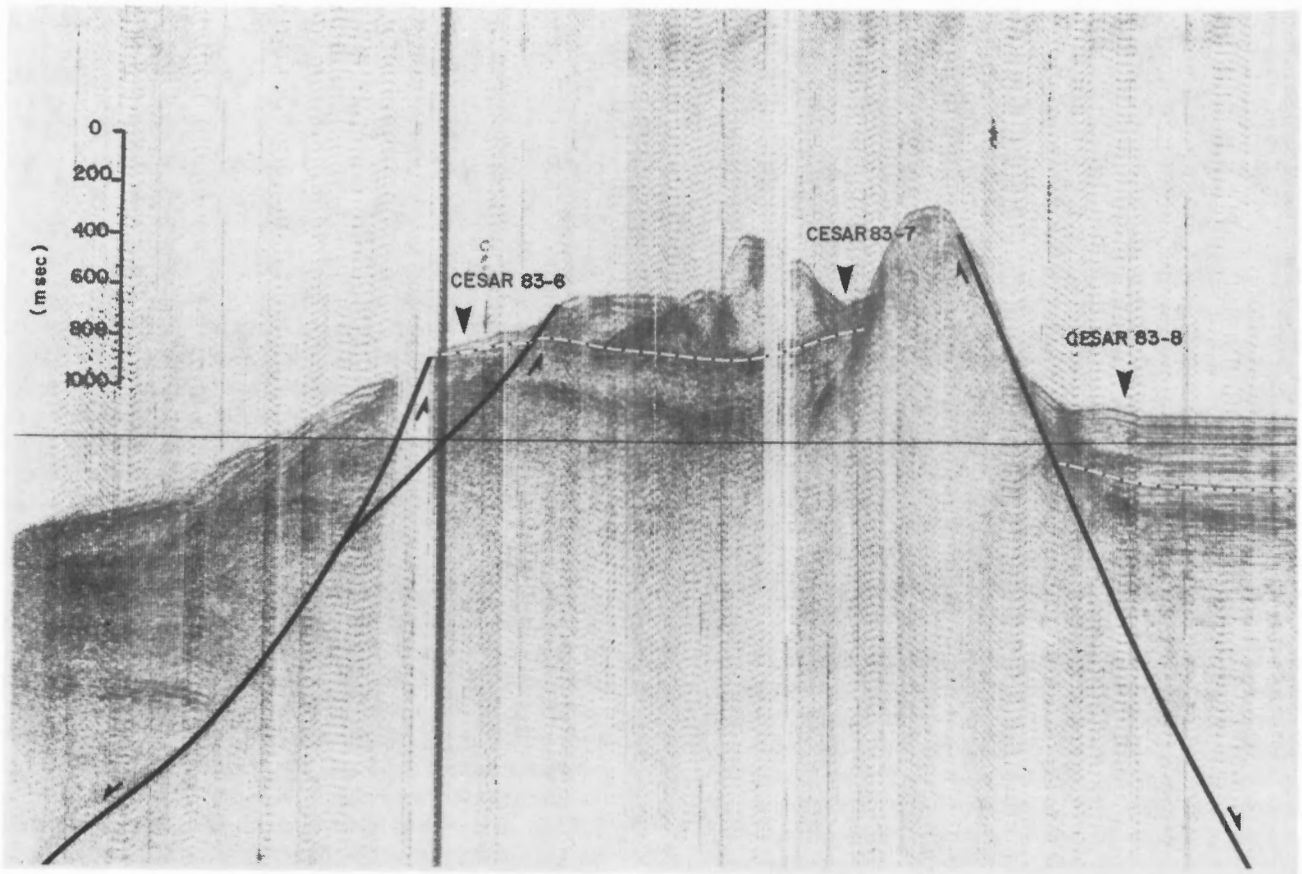

Figure 6.9 Seismic reflection profile of the northern Alpha Ridge crest, showing sediment thickness and the tectonic setting of the CESAR 6 core site (CESAR 83-6). Horizontal distance from CESAR 83-6 to CESAR 83-8 is about 8km.

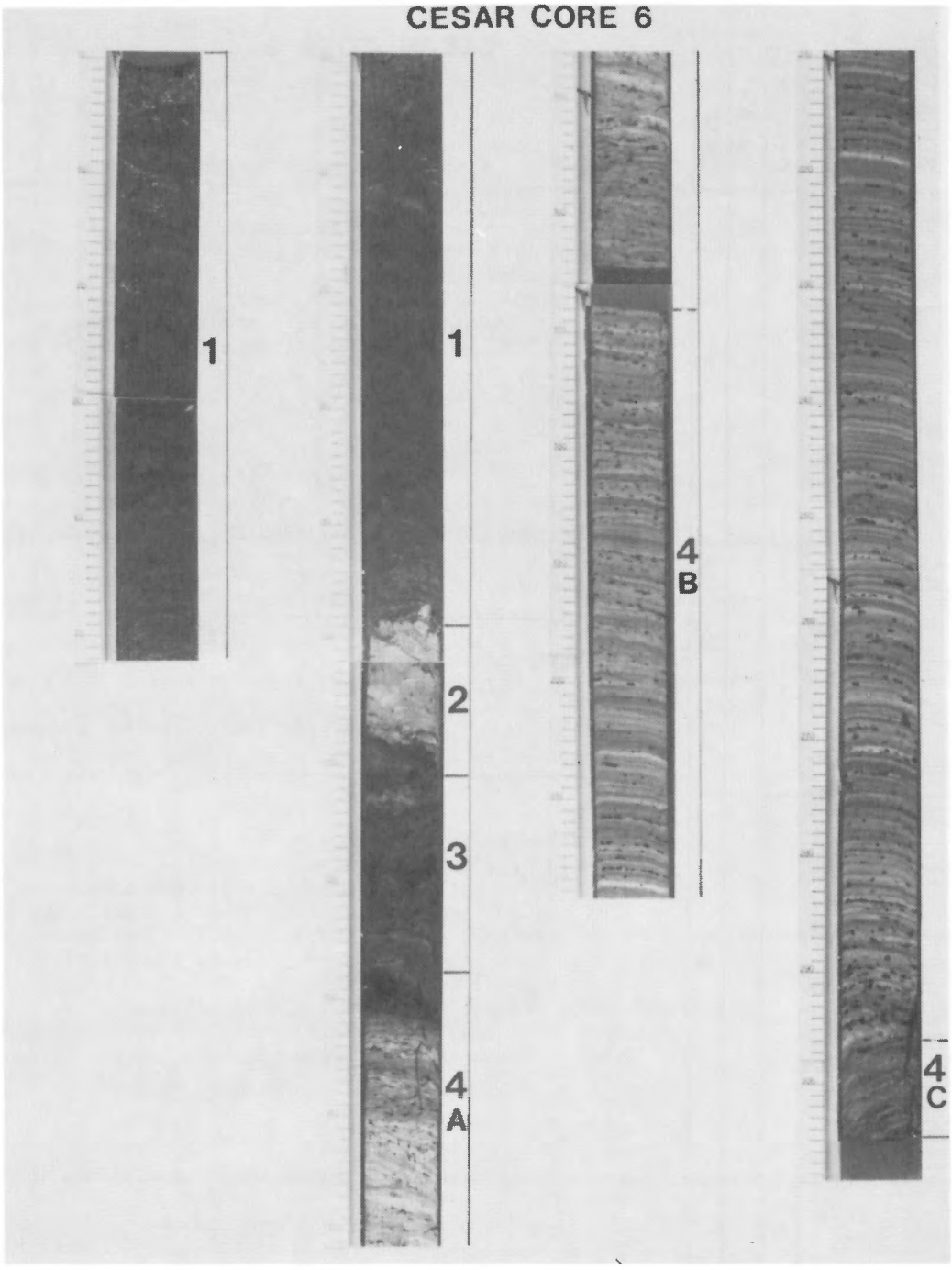

Plate 6.2

Photographic log of sediments in CESAR 6, showing the distribution of lithological units 1 to 4. Vertical scale divisions are in centimetres; note that the numbers at the base of core section 2 (top of column 3) are offset by 3cm – the base of section 2 is at 167.5cm core depth and there is no sediment missing between sections 2 and 3.

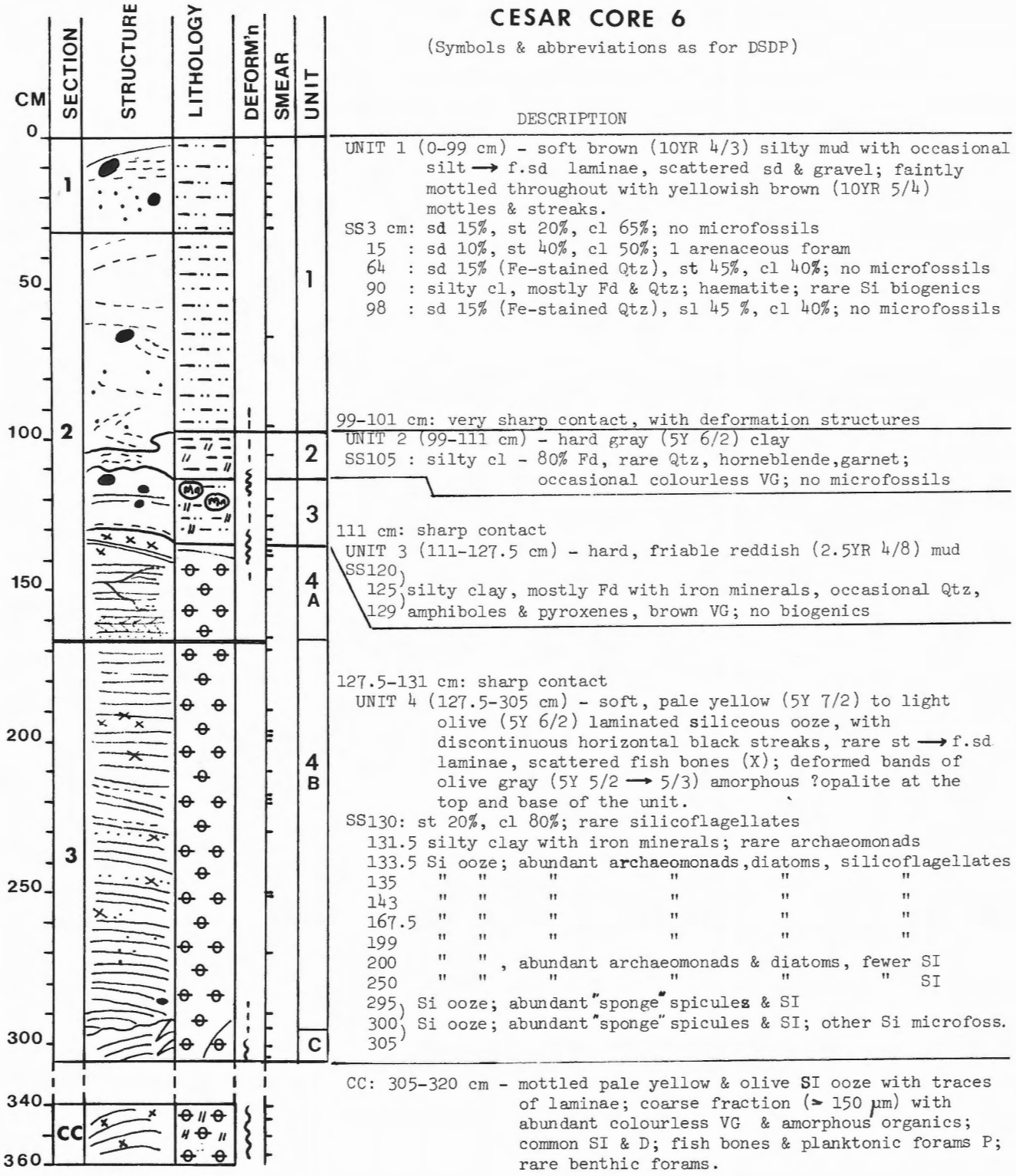

Figure 6.10 Lithological summary of CESAR core 6. Abbreviations used for descriptions: f sd = fine sand; st = silt; cl = clay; Fd = feldspar; Qtz = quartz; VG = volcanic glass shards; SI = silicoflagellates; D = diatoms.

1985) have a Late Cretaceous to Paleogene age but their dark colour suggests they are reworked. Palynomorphs from a bulk sample of surface sediment at site 6 (see Fig. 6.3) indicate a Late Miocene-Pliocene age. The presence of mica and vermiculite in the fine sand and silt-to clay-size fractions of unit 1, and common silt-sized pyroxene suggest an origin from highly weathered volcanic rock, probably including the exposed flanks of the northern Alpha Ridge Crest.

Unit 2 (99-111cm) is a hard grey (5 YR 6/2) silty clay, with sharp but irregular contacts with units 1 and 3. Thin (2-4mm) fractures cut these contacts (probably due to coring disturbances) and are infilled with brown mud. No microfossils or palynomorphs have been found in this unit, and its age is presently unknown. Most of the sediment consists of fine silt-to clay-sized feldspar which is aggregated into sand-sized soft pellets. The mineral composition, in situ colour and texture of this unit suggest that it is a volcanic ash deposited in an oxygen-poor environment. Some colourless volcanic glass is also present (see Fig. 6.10), and rare grains of garnet.

Unit 3 (111-127.5cm) is a hard reddish (2.5 YR 4/8) silty mud with traces of irregular, alternating lighter (10 YR 7/6) and darker (10 YR 5/6) laminae (0.5-2cm thick) from 111-118cm and at the base. The rest of the unit is highly mottled, ranging from small (0.5-1cm) dark brown streaks or black speckles to large (5 × 4cm) dark brown patches with black inclusions. A sharp but irregular contact separates units 3 and 2, and a reddish brown lamina at the base visually suggests a sharp contact at the top of unit 4. However, it is possible that this lamina and the contorted grey and light brown bands of soft sediment from 127.5-133.5cm in unit 4 are part of a gradation from units 3 to 4. Most of the sediment in unit 3 consists of iron-stained, silt-sized feldspar which is loosely aggregated into coarse sand- to granule-sized pellets, the largest of which show faint laminations. Opaque minerals are common, and brown volcanic glass is present. No microfossils or well-preserved palynomorphs are present, therefore the age of this unit is uncertain. The deformed laminae at the top of unit 4, however, show a gradient from occasional well-preserved Late Cretaceous silicoflagellates at 134-130cm to rare fragments at 127-129cm. Some pollen and spores from 127-129cm and 134-136cm have a Paleogene age range (Mudie, 1985) suggesting that the base of unit 3 is not much younger than Late Cretaceous. The mineral composition, colour and structure of unit 3 suggest a volcanic ash deposit similar to that of unit 2 but with oxygen-rich bottom water and a higher influx of ferric hydroxides accounting for the redder colour and higher ferromanganese content (P. Stoffyn, personal commmunication, 1984).

Unit 4 (127.5-305cm) is a soft, laminated, siliceous ooze which contains complex and variable sequences of laminations and microstructures. Most of the unit consists of uncompacted diatomite with a siliceous microfossil content of 80-95%. The lithology, mineralogy and microstructures of unit 4 are described in detail in the next section of this report and the paleomagnetic record of the entire core is described by Aksu (1985a). Bukry (1985) and Barron (1985) document the taxonomy and biostratigraphy of silicoflagellates and diatoms, respectively. Palynomorphs, which are rare in all but the core catcher sediment of CESAR core 6, are described by Mudie (1985). The combined data establish the following facts for CESAR core 6, unit 4.

1. The siliceous ooze is a biogenic marine deposit of Late Cretaceous age, no older than Late Campanian (ca. 73-78 Ma on the time scale of Harland et al., 1982).

2. The paleomagnetic inclination predominantly records a reversed polarity interval, which means that the section was probably not deposited during the Cretaceous "Quiet Interval" (Anomaly 33, from ca. 79-72.5 Ma); therefore, the unit is most likely younger than 73 Ma.

3. The very low concentration of terrigenous clastics in the laminated sediment establishes that the core site must have been isolated from continental sediment sources.

4. The absence of diagenetic alteration of siliceous microfossils from Opal-A to Opal-CT in most of unit 4 establishes that the Cretaceous sediment in CESAR core 6 was never subjected to prolonged heating (>35°C; Siever 1983) or deep burial (>400m; Isaacs 1981).

5. The absence of large-scale sorting and rare breakage of delicately spined siliceous microfossils makes it highly unlikely that unit 4 is a turbidite, gravity flow or slump deposit, although microscale crossbedding and grading features suggest intermittent intervals of current sorting and influx of fine grained turbidites. The complete absence of calcareous microfossils or calcite in unit 4 is unique among all reported laminated siliceous sediments, especially compared to regions of nutrient upwelling where high primary productivity accounts for high rates of biogenic siliceous sediment accumulation.

The apparently unique nature of the Alpha Ridge laminated biosiliceous sediment makes it very difficult to determine what kind of paleoenvironment the Arctic Cretaceous sediments represent. Other short cores of siliceous sediment from the flanks of the southern crest of Alpha Ridge have been interpreted as slide blocks (Clark, 1977) or in situ deposits (Kitchell and Clark, 1982) of pelagic biosiliceous sediment that indicate seasonal very high productivity in a warm Cretaceous-Paleogene Arctic Ocean. Laminae in these cores were not well preserved, however, and this hypothesis must be re-examined in light of the new data on sediment structure, microfossils, palynology, geochemistry, and the paleomagnetic record of the laminated sediments in CESAR 6.

Fine structures and composition of the laminated sediment

The laminated sediments in unit 4 of CESAR 6 can be grouped into 3 subunits based on differences in gross structure and orientation of the laminae. From the base up, the following subunits are distinguished.

Subunit C (305-296cm) This consists of a group of greyish-hued (5 YR 5/2-5 YR 6/3) discontinous laminae which dip at a 30° angle, mostly have indistinct contacts and a mottled appearance, and rarely contain FeMn "micronodules" (small clusters of black particles with a high Fe and Mn content).

Table 6.3 CESAR core 6: organic matter analysis*

Unit	Sample depth (cm)		H%	C%	N%	C/N	H/C
1	5.5 – 8.0	(brown)	0.43	0.07	0.13	0.54	6.14
	89 – 91.5	(brown)	0.53	0.08	0.06	1.33	6.63
2	103 – 105.5	(grey)	0.65	0.55	0.04	13.75	1.18
			0.61	0.20	0.01	20.00	3.05
	105 – 107.5	(grey)	–	0.34	0.54	0.63	–
			0.43	0.45	0.02	22.50	0.96
3	114 – 116.5	A (brown)	0.96	0.05	0.10	0.50	19.2
		B (white)	0.65	0.10	0.17	0.59	6.5
	123 – 125.5	(olive)	0.77	0.11	0.15	0.85	7.0
4	129.5 – 132	A (grey)	1.04	0.21	0.17	1.23	4.95
		B (yellow)	1.26	0.11	0.37	0.30	11.45
	131 – 133.5	(brown)	1.37	0.24	0.05	4.80	5.7
	139 – 141.5	A (olive)	1.03	0.27	0.04	6.75	3.8
		B (white)	1.11	0.69	0.11	6.27	1.6
	146.5 – 149	(pale y)	0.92	0.29	0.52	0.56	3.17
	186 – 188.5	A (grey)	0.90	0.55	–	–	1.64
			0.44	0.68	–	–	0.65
		B (pale y)	1.19	0.43	2.37	0.18	2.77
	214.5 – 217	A (yellow)	1.05	0.34	0.85	0.40	3.08
		B (pale y)	1.09	0.47	0.17	2.76	2.32
			1.01	0.20	0.16	1.25	5.05
		C (bn-y)	0.99	0.19	0.44	0.43	5.21
			1.05	0.27	3.19	8.46	3.89
	217 – 219.5	A (white)	1.05	0.23	0.92	0.25	4.57
			1.05	0.25	0.75	0.33	3.20
		B (white)	1.04	0.16	0.41	0.39	6.50
			1.04	0.24	0.05	4.80	4.33
		C (yellow)	1.09	0.40	0.77	0.52	2.73
			1.09	0.39	0.49	0.80	2.79

*C, H and N were measured using a Perkin-Elmer model 240B elemental anlayzer.

Subunit B (296-167cm) This consists of very regular, thin (2cm) pale yellow (5 YR 7/4) to olive (5 YR 5/4) or brown (10 YR 5/6) laminae which dip 10-20° in the opposite direction to subunit C, often have sharp contacts, and are frequently speckled by small (2-4mm) FeMn "micro-nodules" which often occur as short bead-like chains.

Subunit A (167-127.5cm). From the base upwards, this unit consists of the following sequence: i) 8cm of olive (5 YR 5/4) to brownish-yellow (10 YR 6/6) irregular laminae with mostly graded contacts and a faintly crossbedded structure; ii) ca. 12cm of lighter (5 YR 6/2-6/4) laminae with sharpish bases, variable thickness (from 0.5-3cm) and irregular orientation due to areas of slip-strike displacement (ca. 2 cm) along microfaults; and iii) a 20cm section of thickish (2-3cm), light olive (5 YR 6/2) to dark yellowish-brown (10 YR 3/4) mottled laminae which are primarily flat-lying but become strongly deformed in the top 7cm. FeMn mottles or streaks are common throughout this subunit.

Very detailed, lamina-by-lamina textural, mineralogical and geochemical studies are required to understand the nature and probable causes of these meso- and micro-scale changes in unit 4. Preliminary studies have been carried out for selected samples, using smear slides, organic matter (CHN) analysis (Table 6.3), scanning electron microscopy (SEM), Energy Dispersive System (EDS) element analysis and visual inspection of the coarse (125μm) sediment fractions. The main results are described below.

Subunit C (305-296cm). Studies of light and dark lamina couplets from 305cm and 301.5-304cm show that:

1) Light and dark laminae differ mainly in the larger amount of iron oxyhydroxides and bone fragments present in the dark laminae (see Plate 6.3, fig. 1 and 2; Plate 6.4, fig. 1).

2) There is no conspicous difference in silicoflagellate or diatom composition between light and dark laminae within the subunit.

3) There are no conspicous differences in preservation state of siliceous microfossils between light and dark laminae, although there are more brown-stained *Coscinodiscus* with thin coatings of Fe in the dark laminae (see Plate 6.4, fig. 3, 5 and 6).

In general, thin rod-shaped biosiliceous fragments are much more abundant in subunit C than elsewhere in unit 4. The siliceous rods appear to reflect the frequent occurrence of *Rhizosolenia cretacea*, presence of several *Lyramula* species in addition to ubiquitous *Lyramula deflandrei*, and perhaps (not yet confirmed), the presence of sponge spicules. The top of the subunit corresponds to the last occurrences of *Lyramula minor, Lyramula porta* and *Lyramula* spp. (see Bukry, 1985), the last occurrence of *Coscinodiscus symbolophorus*, and a change from common or frequent *Rhizosolenia cretacea* and *Hemiaulus polymorphus* v. *frigida* to very rare occurrences (see Barron, 1985). Ferromanganese "micronodules" are very rare and small (<20μm) throughout the subunit, whereas larger, dark brown grains of iron-stained apatite ($CaPO_4$) are relatively common, some irregular shaped $CaSO_4$ particles are present, and some siliceous microfossils show patchy overgrowths of $CaSO_4$ (Plate 6.4, fig. 5).

It is not clear if the changes at the top of subunit C represent an unconformity or disturbance during coring. The laminae at the bottom of subunit B are strongly bowed upwards, suggesting partial flow-in which might account for the rare occurrence of *Lyramula furcula* at 290-292cm, but most of the diatom species are the same in subunits C and B. In general, it appears more likely that the subunits represent a change in frequency of clay and iron-rich mineral influx, and a change in sediment bottom water chemistry as indicated by the more common occurrence of FeMn deposits in subunit B.

Subunit B (296-167cm). Despite the ostensibly regular appearance of laminae in this subunit, detailed study reveals complex and variable microstructures which make it difficult to characterize either dark-light laminae couplets or lamina sets. This difficulty is due to 3 main factors: a) colour changes cover a spectrum from sharply defined couplets of very dark and very light laminae to graded sets in which the colour changes gradually from darker to lighter and back to darker (see Plate 6.2); b) X-radiograph microstructures (Plates 6.5 to 6.8) mostly do not correspond directly to conspicuous differences in lamina colour; and c) there are no obvious differences in microfossil concentrations, size, shape or species composition between light and dark laminae.

In order to try and discern repetitive patterns in the rhythmites of subunit 4B, laminae were mapped on a millimetre by millimetre scale from colour photographs, using different colours to characterize brown (10 YR 5/6), olive (5 YR 5/4) and pale yellow (5 YR 4/4) laminae. This procedure revealed 5 categories of lamina sets which correspond to 5 of 10 lamina types described in the literature on laminated siliceous sediments (Fig. 6.11). Four of these categories correspond to units in chert beds studied by Iijima and Utada (1983); for convenience these are referred to here as 'single layered', 'triple layered', 'laminar' and 'striped'. The fifth category corresponds to turbidite-derived rhythmites described by Nisbet and Price (1974) which are referred to here as 'cross-stratified'. Using the symbols shown in Figure 6.11, the distribution of the rhythmite units from 288-160cm in subunit 4B is mapped in Figure 6.12 and 6.13. The major features revealed by the maps are outlined as follows.

1. There is a gradual change from a prevalence of striped (δ-type) and single (α-type) beds in the lower one-third of subunit 4B (289-250cm, Plate 6.5), to a prevalence of triple-layered (β-type) and laminar (λ-type) beds in the middle section (250-ca. 181cm, Plate 6.6), and a prevalence of crossbedded sets at the top of subunit B (181-167cm, Plate 6.7). The change in prevalent lamina type at 250cm roughly corresponds to the boundary between silicoflagellate zones A3 and A2 described by Bukry (1985), with *Vallacerta siderea* dominating alone in A3 and *Lyramula burchardae* becoming co-dominant with *Vallacerta siderea* in the upper (A2) biostratigraphic unit.

2. The striped beds (δ-type) range in thickness from 5-7cm at the base of the subunit (e.g. Plate 6.5, 289-275cm) to 2cm above 250cm-depth. Below 250cm, each bed is characterized by a brown lamina at the base which grades to, or is abruptly followed by a series of 5-7 alternating pale yellow and olive laminae, with either sharp or wispy contacts. X-radiographs show that the brown laminae correspond to relatively fine grained muddy layers, which often show very faint lighter and darker silt-clay couplets (ca. 2mm thick) and sometimes have a sharply defined dark-light couplet at the base. The yellow and olive laminae are either structureless, or they contain wispy light-dark microlamina couplets (ca. 1-2mm thick) with graded, or rarely, sharp contacts. Smear slides indicate that the brown laminae contain more clay-size particles than the pale laminae; the latter contain abundant large flocs of biosiliceous material and many cylindrical diatoms.

3. The single beds (α-type) range in thickness from ca. 4-10mm; X-radiographs (Plate 6.5, 263-260cm) show that they are mostly weakly graded, with a sharp, thin (1mm) light-dark microlamina couplet at the base or top.

4. The triple-layered beds (β-type) range in thickness from ca. 1-2cm and are characterized by a brown lamina at the base and top, both of which grade to pale yellow or olive in the centre. X-radiographs (e.g. Plate 6.6, 241-239cm, 234-231cm) show that the brown laminae are muddier, with wispy dark-light microlamina couplets ca. 1mm thick; the light coloured laminae contain denser sediment and wispy microlaminae 2-3mm thick. Smear slides, EDS analysis, and SEM studies (Plate 6.9) show that the brown and olive-brown layers contain common sand-size particles of $CaPO_4$ (probably bone) and clay-size particles containing Fe and Al in addition to abundant biosiliceous material. The white layers contain bone fragments but clay and metallic minerals are rarely detectable in the biosiliceous sediment (P. Stoffyn, personal communication, 1984). Large flocs of biosiliceous material are common in the white laminae (Plate 6.9, fig. 1). In both light and dark laminae, fine grained particulate FeMn occurs in patches resembling small burrows. Overgrowths of Mn were found on some diatoms (Plate 6.9, fig. 8).

5. The laminar beds (λ-type) in subunit 4B range in thickness from 2-10cm, and consist of sets of 3-10 alternating dark and light layers with sharp contacts. The dark-light pairs are variable in thickness, ranging from a thin (1mm) dark lamina and thicker (4mm) white lamina to dark-light layers

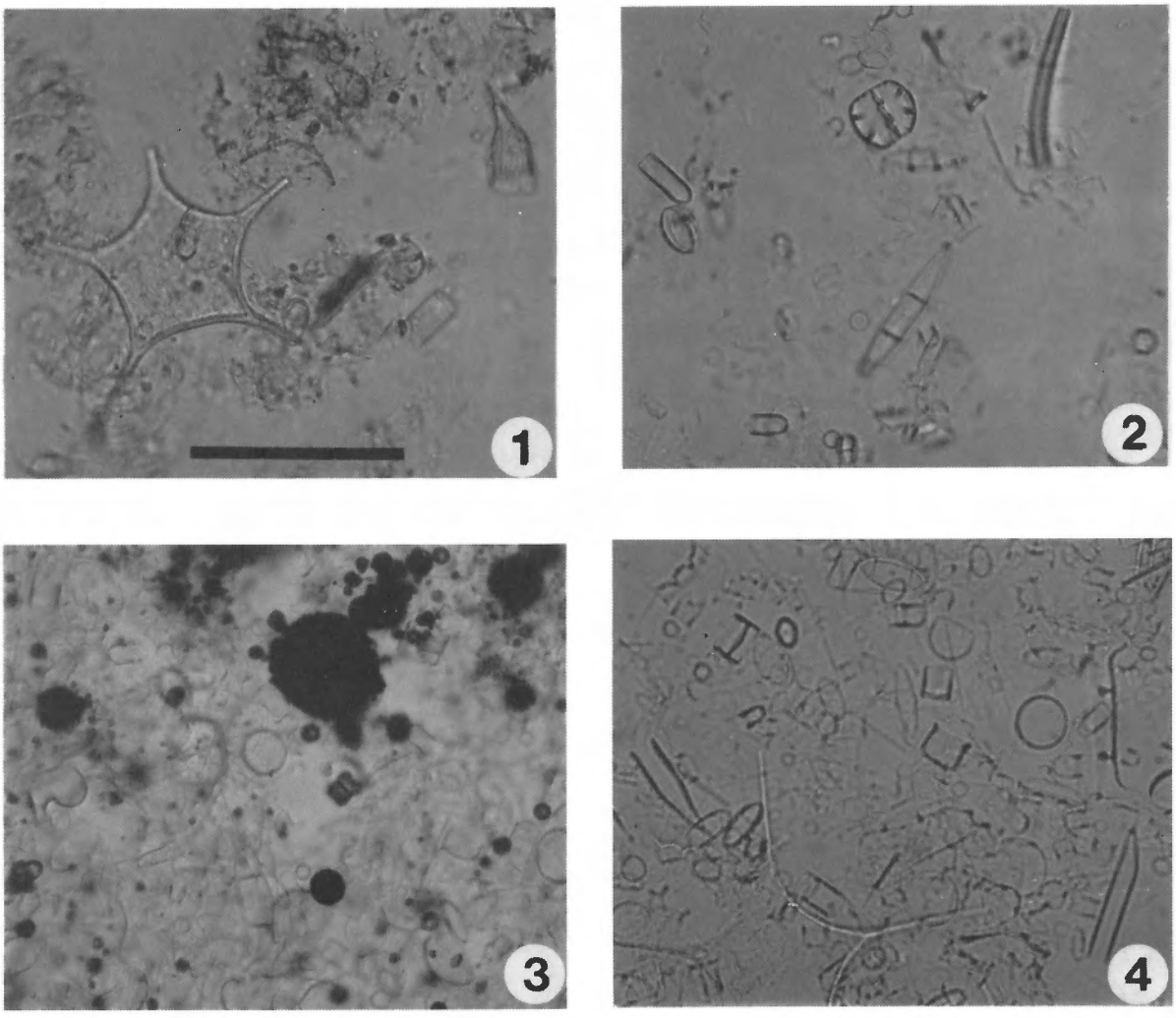

Plate 6.3

Smear slide samples of sediment from CESAR 6; light photomicrographs × 400; # = photo negative; bar scale = 50 μm.

Figure 1 Brown lamina at 305cm, showing *Vallacerta siderea* and *Rhizosolenia* sp. (thick form) in loose aggregates of silt – clay sized particulates with common small diatoms and resting spores (# 830613-3).

Figure 2 White lamina at 305cm, showing *Rhizosolenia cretacea, Anaulus sibericus, Hemiaulus* valves and many small diatoms. Note the absence of clay and mineral aggregates (# 830613-2).

Figure 3 Black micronodule at 226cm, showing FeMn particles in a dense matrix of small diatoms and resting spores (# 840126-3).

Figure 4 White lamina at 226cm, showing *Vallacerta siderea, Rhizosolenia* sp. (thin form) and abundant diatoms, resting spores and thin biosiliceous rods (# 840126-7).

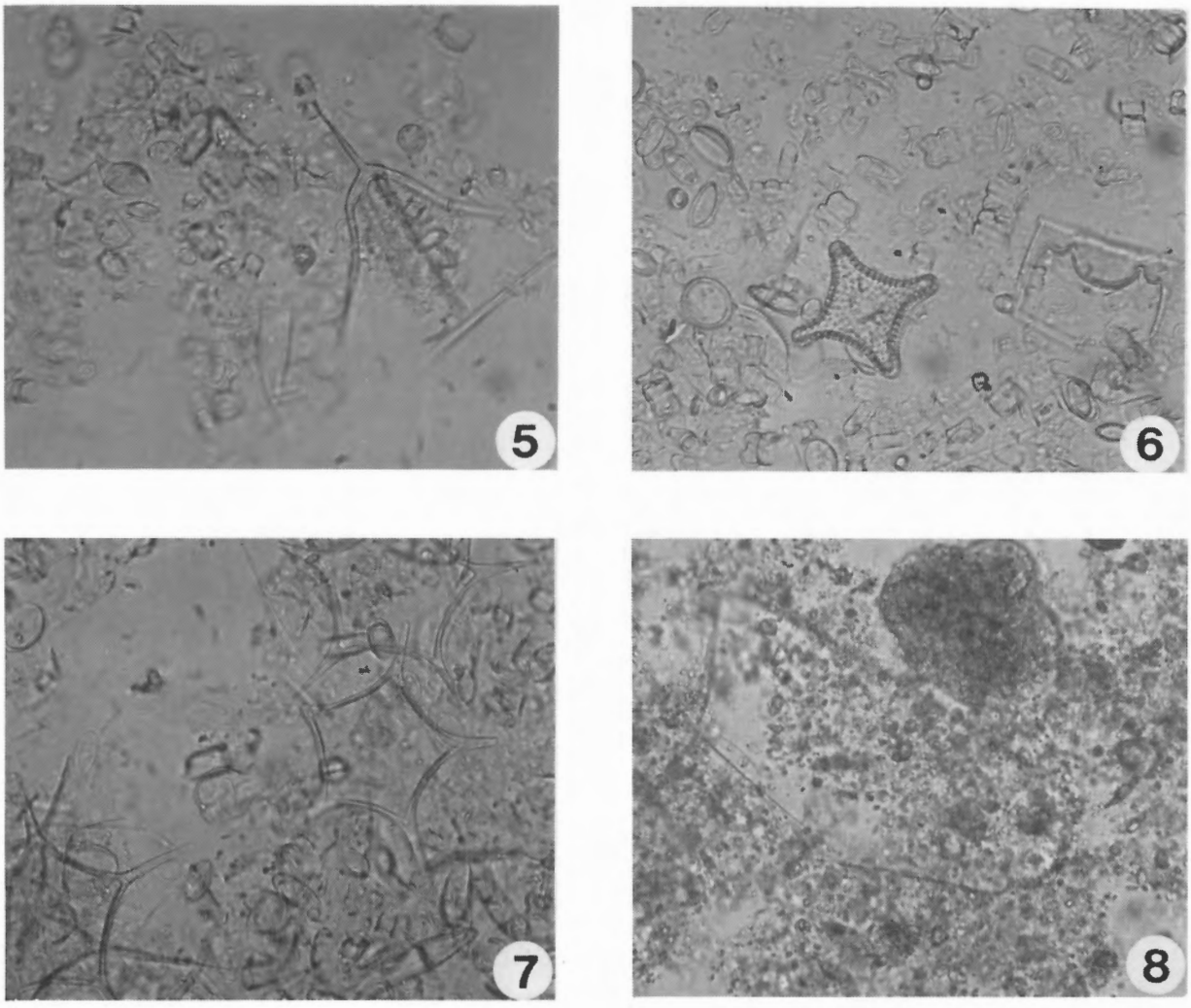

Plate 6.3 (cont'd)

Figure 5 Brown lamina at 167.5cm, showing *Lyramula burchardae, Rhizosolenia* sp. and abundant small diatoms in a loose matrix of silt – clay sized particulates (# 830613-6).

Figure 6 White lamina at 167.5cm, showing *Triceratium tessela, Hemiaulus* and *Skeletonema* valves and traces of diatom plus particulate Fe agglomerates (# 830613-4).

Figure 7 Pale brown lamina streaked with FeMn particulates at 137.5cm, showing *Vallacerta siderea* and abundant small diatoms in a dense matrix of silt – clay sized particulates (# 830613-8).

Figure 8 Grey, semiconsolidated, sandy mud at 106cm, showing volcanic glass shard, sand pellet, and silt to clay-sized feldspar grains (# 830613-7).

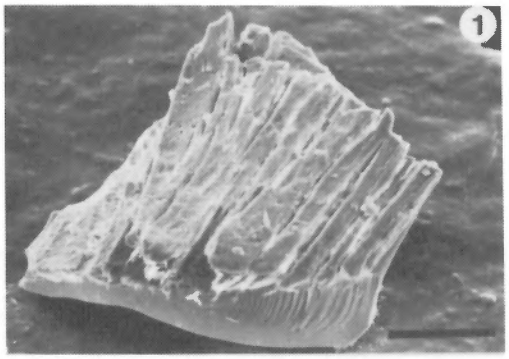
1

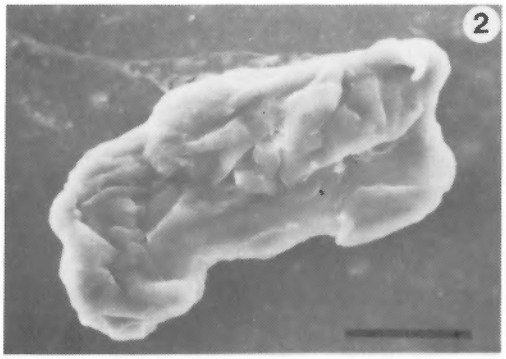
2

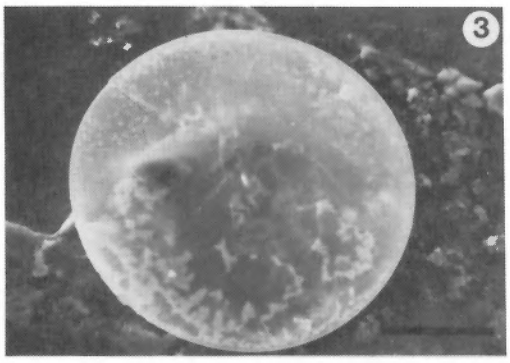
3

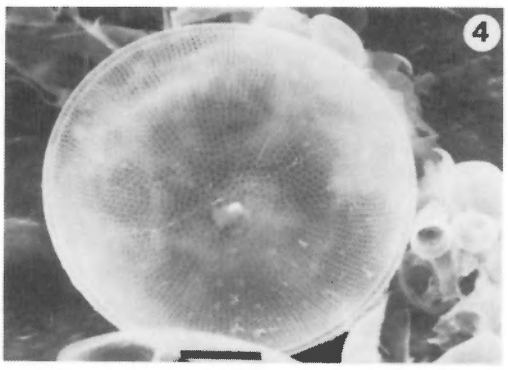
4

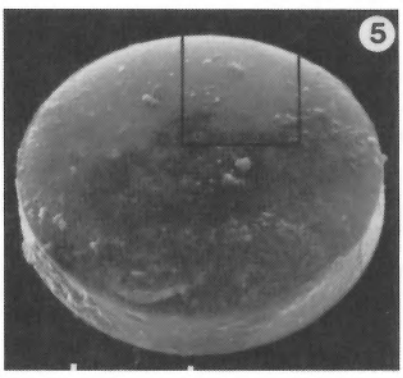
5

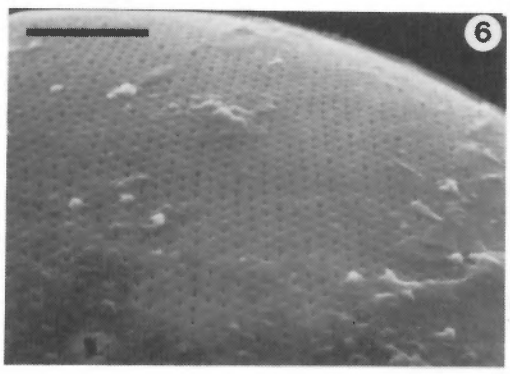
6

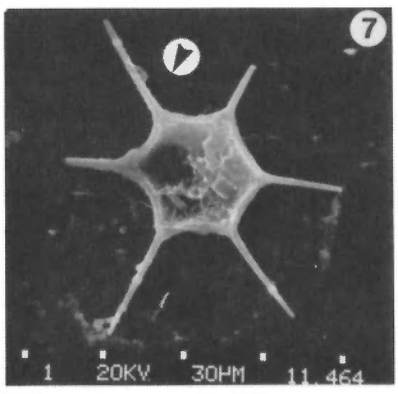
7
1 20KV 30PM 11.464

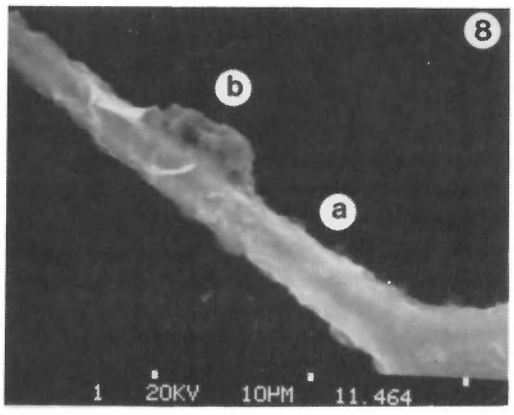
8
b
a
1 20KV 10PM 11.464

each of which is ca. 1cm thick. X-radiographs (e.g. Plate 6.7, 206-198cm) indicate that the brown laminae contain more clay than the light laminae, and they show wispy dark-light microlamina couplets, ca. 2mm thick. The denser, light-coloured laminae are unstructured and faintly mottled or show very wispy microlaminae. Smear slides (Plate 6.10) show that there is very little difference in the microfossil content of the dark and light laminae.

6. The cross-stratified sets (χ-type) resemble those characterizing turbidite-derived laminated beds in the Neraida chert member of the Agrilia Formation in Greece (Nisbet and Price, 1974), but they do not always show a distinct structureless sandy silt layer at the base. In unit 4, each set usually consists of a basal muddy brown lamina 1-2cm thick which is faintly parallel laminated in X-radiographs (e.g. Plate 6.7, 178-167cm), followed by 1-2 cm of 20-30° dipping cross laminae. These beds are cut by a parallel laminated muddy brown layer at the top, followed by a structureless light-coloured lamina of biogenic silica.

Subunit A (167-127.5cm). Cross-stratified laminae similar to those described above are found from 167-159cm. From 159 to 153cm, the laminae are generally sharp-based and have graded contacts between light and dark couplets. From 153-134cm, distinct laminae cannot be delimited although wispy, thin light-dark couplets can be seen in X-radiographs (Plate 6.8). Subparallel, elongated mottles rich in FeMn also become conspicuous in this interval which corresponds to the top silicoflagellate zone (A1) of Bukry (1985). The top of subunit A (Plate 6.8) is marked by relatively thick (2-3cm), heavily mottled laminae with scattered, well-preserved, small fish bones. Traces of microlamina couplets can be seen in places. No identifiable microfossils are present above 132cm core depth; however, palynomorphs are fairly common, and clay minerals and iron flocs increase in frequency.

Paleoenvironmental interpretation

Kitchell and Clark (1982) and Clark (1977) have postulated that the Alpha Ridge biosiliceous deposits reflect seasonally high productivity in a warm ocean with wind-driven cyclonic circulation and polar upwelling. According to Barron (1985), this hypothesis now is further supported by lack of evidence for major diatom evolutionary changes in the CESAR laminated sediments, which may indicate that a relatively short time interval and high rate of deposition is represented. However, the low diversity of siliceous microfossil species and present sparse knowledge of Cretaceous high latitude marine floras makes this judgment difficult to evaluate (see Bukry, 1985). The problem is further confounded by evidence for strong provincialism in the Late Cretaceous-Paleogene marine flora and fauna (Marincovich, et al., 1983). Furthermore, the upwelling hypothesis suffers greatly from the remarkable absence of calcareous microfossils and dinoflagellates, both of which are normally associated with high organic productivity and seasonal upwelling. The presence of penecontemporaneous foraminiferal and dinoflagellate deposits in the Kanguk Formation of the Canadian Arctic Islands (Miall, 1979; Plauchut and Jutard, 1976) seems to eliminate the likelihood that the absence of these microfossils in Alpha Ridge sediments was due to their lack of occurrence in the Cretaceous Arctic Ocean. A more likely explanation seems to be that the Alpha Ridge depositional environment was unfavourable for the preservation of calcareous and organic-walled microfossils.

Plate 6.4 (opposite)

Scanning electron microscope (SEM) photographs of minerals and siliceous microfossils in a brown lamina in subunit C (302.5cm) or a white lamina in subunit B (211cm) of CESAR 6. SEM photos by B. Deonarine, AGC.

Figure 1 Dark brown mineral from 302.5cm, composed of $CaPO_4$ with surface flakes containing Na, Cl and S; laminated structure suggests a fish otolith. AGC # 1146.9; bar = 100μm.

Figure 2 Glassy white mineral composed of $CaSO_4$, from 302.5cm. AGC # 1146.6; bar = 30μm.

Figure 3 Surface view of semitranslucent white valve of *Coscinodiscus circumspectus* from 302.5cm, showing thin patchy coating containing Si, Na, Cl and Ca. AGC # 1146.1; bar = 30μm.

Figure 4 Surface view of translucent white valve of *Coscinodiscus circumspectus* from 211cm, showing lack of surface mineral coating. AGC # 1139.2; bar = 10μm.

Figure 5 Oblique surface view of a dark brown specimen of *Coscinodiscus circumspectus* from 302.5cm, showing the heavy coating of material containing Si, Ca, S, K and Cl; black lines delimit area enlarged in figure 6. AGC # 1146.2; scale marks = 30μm.

Figure 6 Enlargement of area outlined in figure 5, showing fine detail of pores and the edge of the mineral coating. AGC # 1146.3; bar = 10μm.

Figure 7 *Vallacerta siderea* (6-spined form) from 302.5cm, showing a patchy coating of minerals containing Si, Ca, P and S. AGC # 1146.4; white squares along bottom delineate 30μm scale intervals.

Figure 8 Enlargement of spine base indicated by arrow in figure 7, showing "clean" area containing only Si mineral, and warty area containing Ca, S and Si. AGC # 1146.4; white squares along bottom delineate 10μm intervals.

Plate 6.5, 6.6, 6.7 and 6.8

Photoprints of X-radiographs of CESAR 6, split core halves. Darker and lighter horizontal lines indicate denser and less dense sediment, respectively. Small black speckles are FeMn "micronodules" and burrow linings or fish bones. Very bright white lines are air-filled cracks.

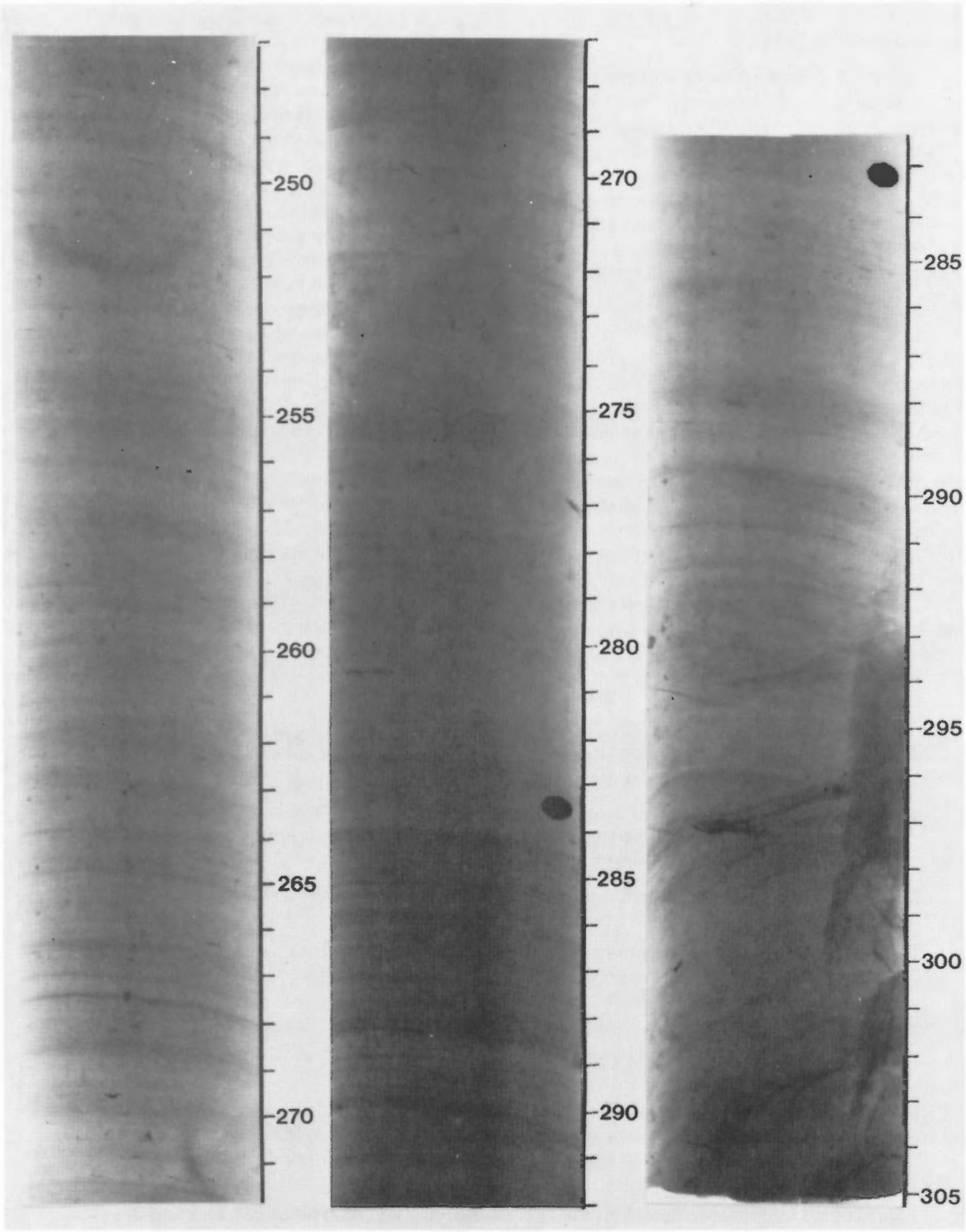

Plate 6.5

247-305cm core depth; vertical wedges from 290-305cm are probably flow-in features.

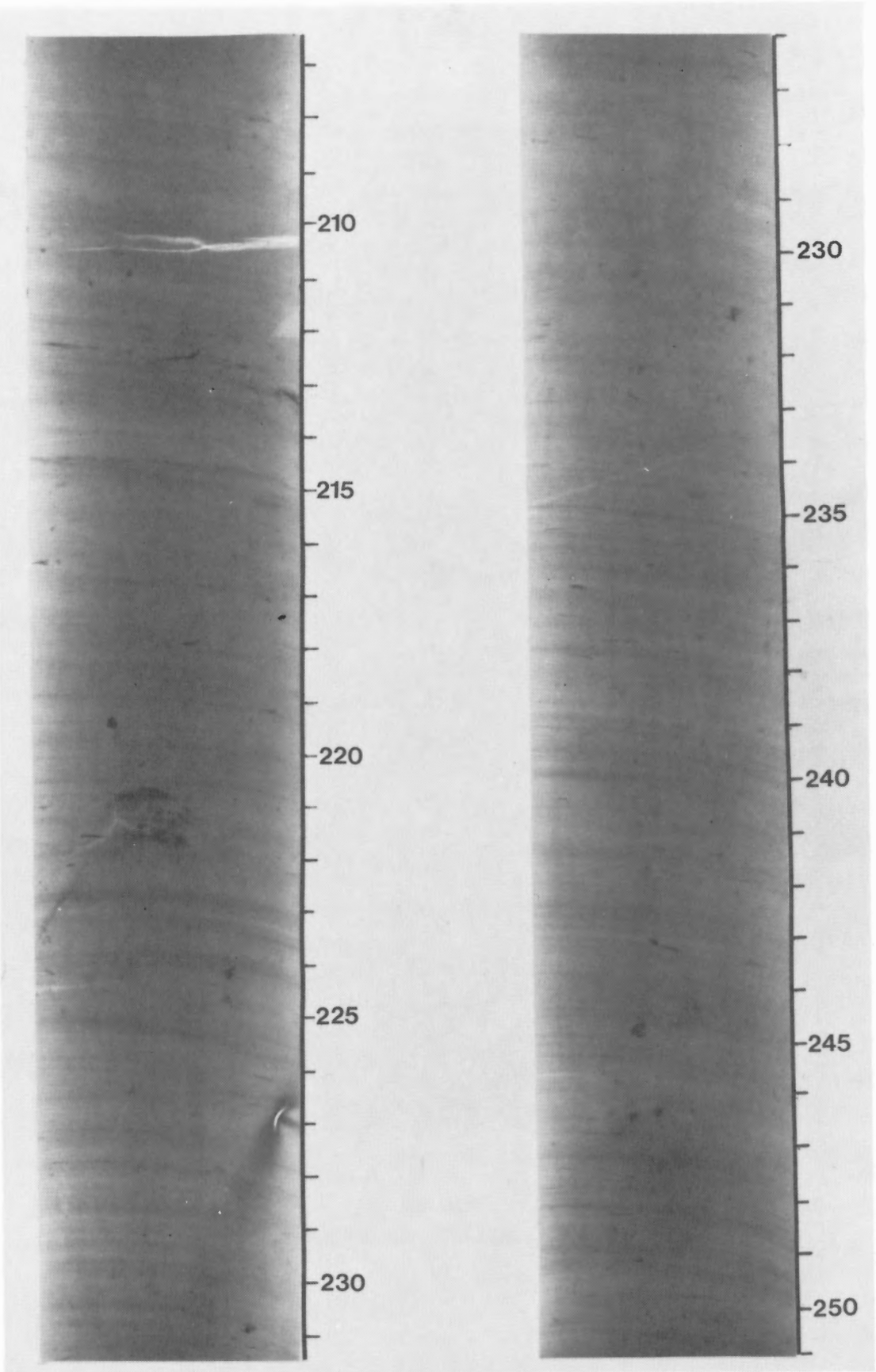

Plate 6.6

251-207cm core interval.

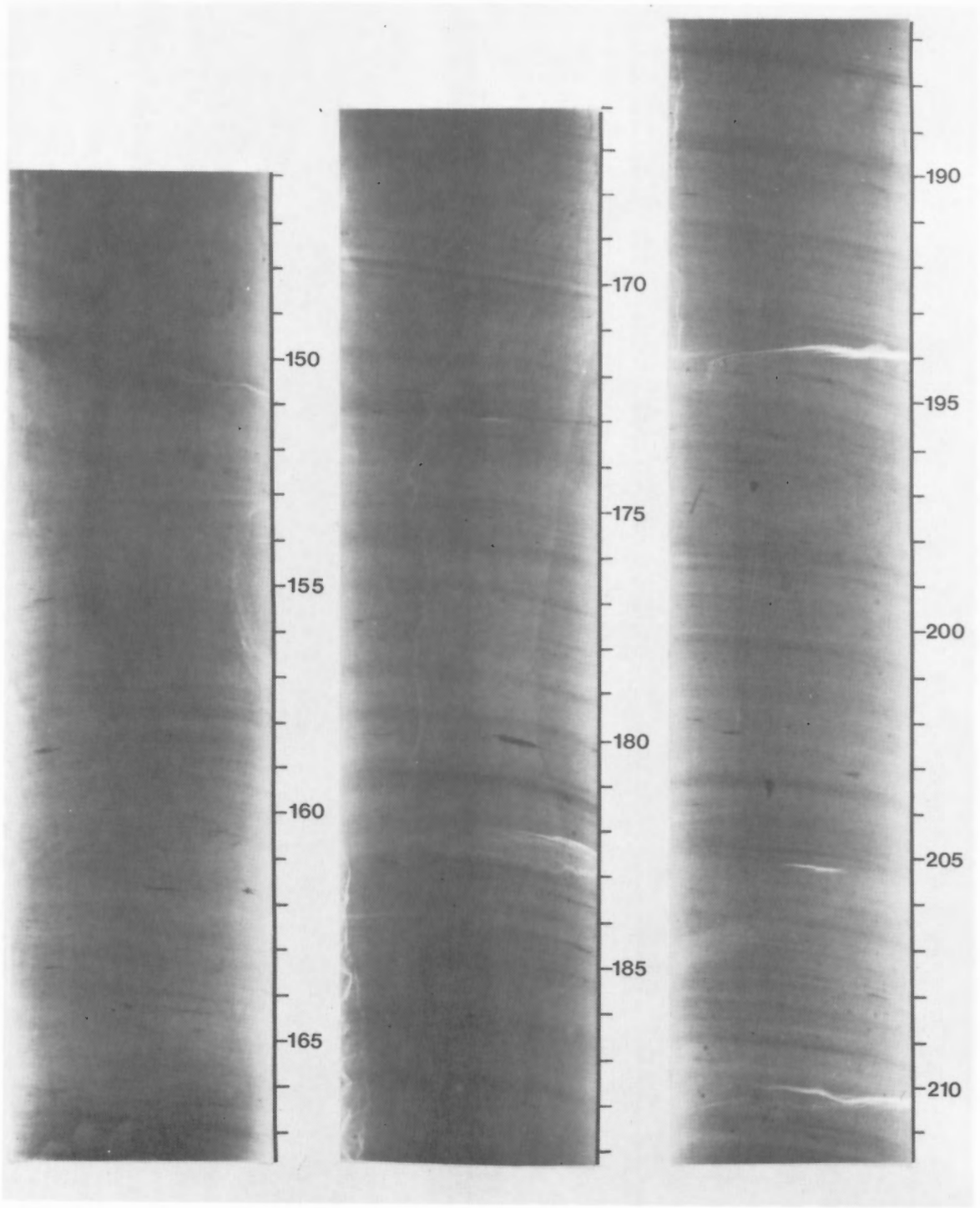

Plate 6.7

211-146cm; long vertical smears mark surface identations caused during core splitting.

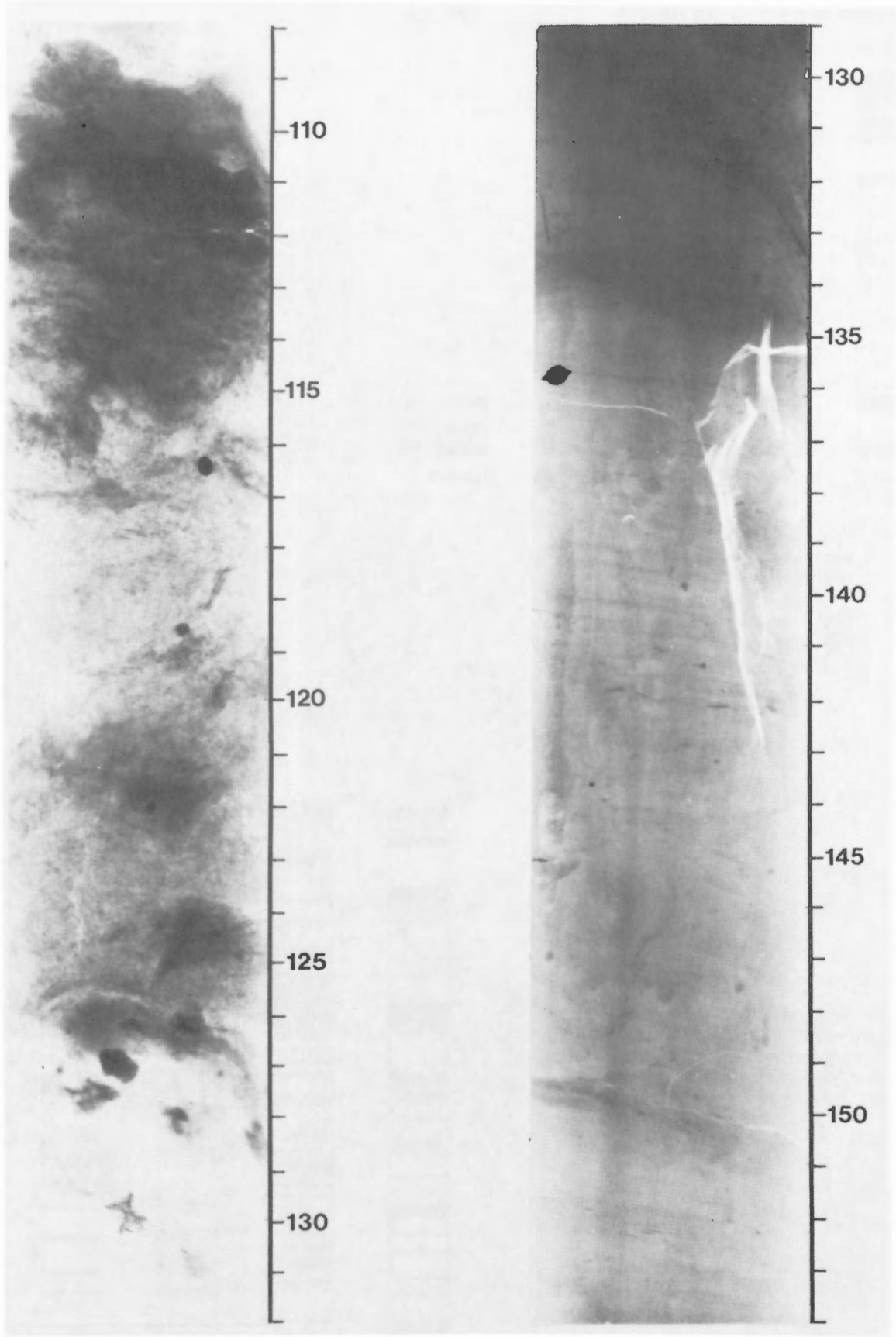

Plate 6.8

154-108cm core depth; photo on right was taken with a short exposure time to emphasize fine laminae below 135cm; photo on left was exposed longer to emphasize medium density sediment components, e.g. the fish vertebra at 130cm.

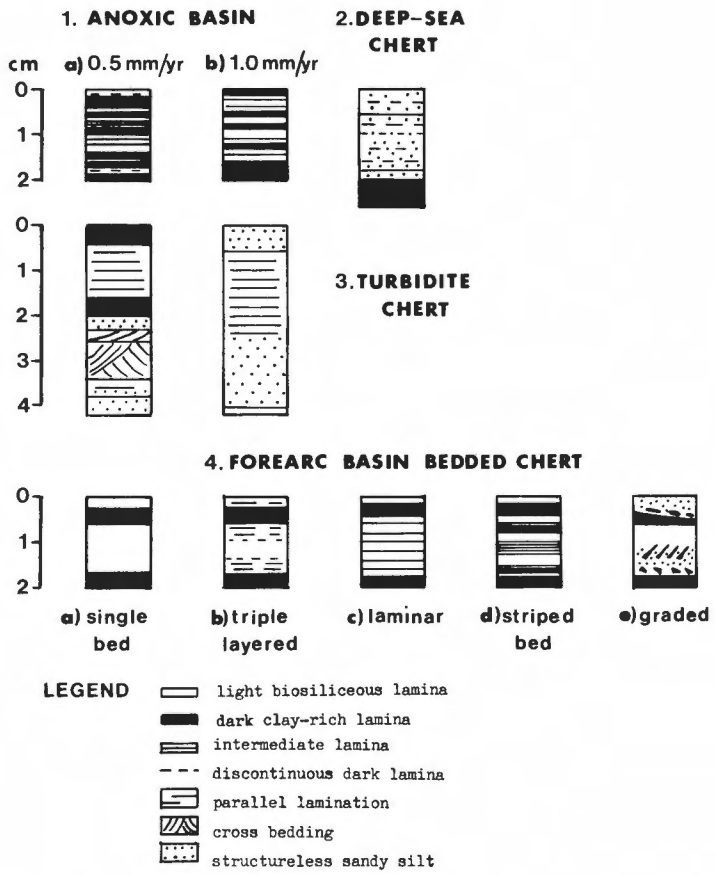

Figure 6.11 Lamina sequences characterizing biosiliceous marine sediments of various depositional environments. 1a – Cariaco Trench, 900m (Heezen and Hollister, 1971, p.224); 1b – Guaymas Basin, 675m, DSDP site 480 (Soutar et al., 1982); 2 – N. Pacific deep-sea bedded chert and shale (Hein and Karl, 1983) and Cretaceous black shale (Thiede et al., 1982); 3a and 3b – Agrilia Formation biosiliceous turbidites (Nisbet and Price, 1974); 4a-4e – Japanese Island forearc basin bedded cherts (Iijima and Utada, 1983).

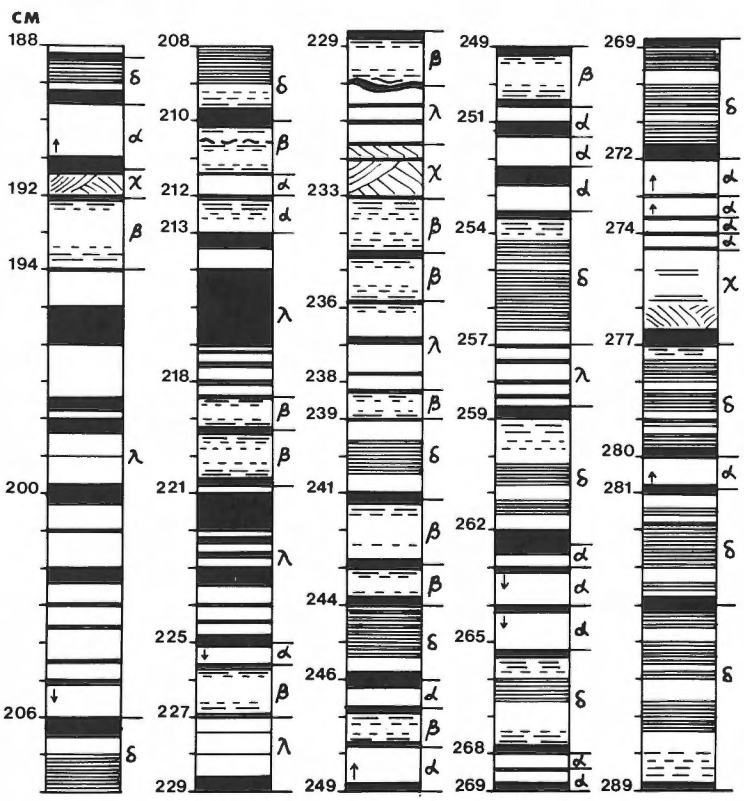

Figure 6.12 Map of lamina sets in subunit B, CESAR 6, from 289-188cm core depth (see Fig. 6.11 for lithological description). Greek letters refer to types of lamina beds described in the text; arrows indicate grading.

Berger and Winterer (1974) have presented strong arguments to the effect that absence of calcareous microfossils in deep sea sediments almost invariably indicates one or more of the following conditions: a) deposition below the CCD (calcite compensation depth) which ranges from ca. 1-4km in the present global oceans; b) lack of calcium supply; c) postdepositional dissolution. With regard to CESAR 6, the high proportion of diatom resting spores in unit 4 implies a relatively shallow water, upper continental slope or offshore bank environment (Barron, 1985), and this interpretation is further supported by the similarity of diatom taxa (Vincent et al., 1983) and silicoflagellates (Bukry, 1981) in the Kanguk Formation of the Canadian Arctic. If primary productivity was extraordinarily high and calcium supply was also limited, it is possible that the Cretaceous CCD was shallower than 1365m (present water depth of CESAR 6) in the Arctic Basin. However, the common presence of calcium phosphate deposits in the CESAR 6 rhythmites argues against an inadequate supply of calcium, especially if seasonal upwelling were to take place. The absence of arenaceous foraminifera is also inconsistent with a productive boreal marine environment. This leaves postdepositional dissolution as the most likely explanation for the lack of calcareous microfossils.

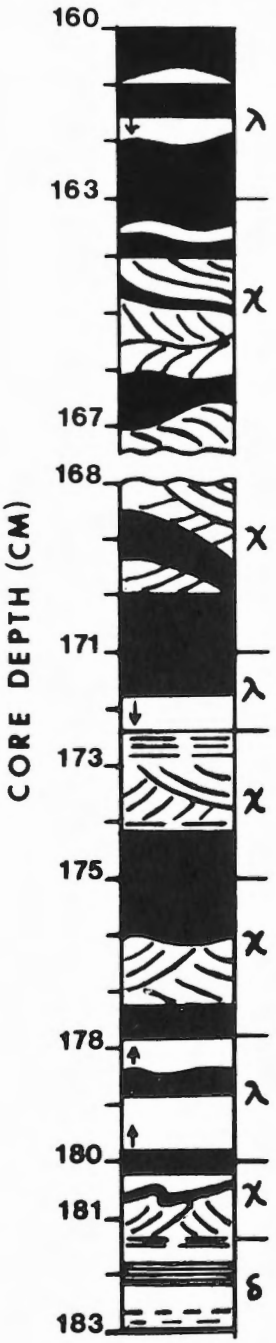

Figure 6.13 Map of lamina sets at the top of subunit B (183-188cm) and the base of subunit C (167-160cm), CESAR 6 (see Fig. 6.10 for lithological description). Greek letters refer to types of lamina sets described in the text; arrows indicate grading.

The possibility of postdepositional calcite solution is given further weight by a) presence of $CaSO_4$ crystals in some laminae, b) the common occurrence of FeMn particulates which indicate an intermittently oxidizing environment, and c) the presence of Fe-infilled foraminiferal linings in some samples (see Mudie, 1985). Slow oxidation of FeS in the presence of oxygen is known to cause dissolution of both calcareous and agglutinated foraminifera (Schnitker et al., 1980). Prolonged oxidation would also account for the destruction of dinoflagellates and other palynomorphs, hence accounting for their rare occurrence in the laminated sediment of CESAR 6, whereas a shallow CCD would not explain this feature.

In conclusion, the combined evidence from sediment structure, texture, microfossils, palynomorphs and limited geochemical data point towards the likelihood that the Cretaceous depositional environment of CESAR 6 was a shallow water offshore basinal environment in a marginal sea, analagous to the Upper Triassic bedded chert deposits in the forearc basins of the Japanese Islands (Iijima and Utada, 1983). Sedimentation rates in these Triassic basins (after decompaction of the cherts) was high: ca. 10mm/1000 yrs. A similar sedimentation rate for Alpha Ridge would mean that unit 4 represents an interval of about 150,000 years. This small amount of time, however, is not in accord with the palynostratigraphy (see Mudie, 1985) or with the paleomagnetic record for CESAR 6 (see Aksu, 1985a), both of which suggest a time-framework of several million years. Hence, it seems more likely that primary productivity and biogenic sediment accumulation in the high latitude (ca. 75°N) Late Cretaceous Arctic Ocean was much lower than in the Pacific island-arc region. Furthermore, according to Berger and Roth (1975), biosiliceous deposits intercalated with phosphatic fossils and apatite indicate low fertility oceanic conditions. Slow deposition in a nutrient-poor, offshore basinal environment, with intermittent influxes of metallic minerals from the Alpha Ridge crest, presently best accounts for the absence of foraminifera, radiolarians and dinoflagellates in the laminated sediments of CESAR 6.

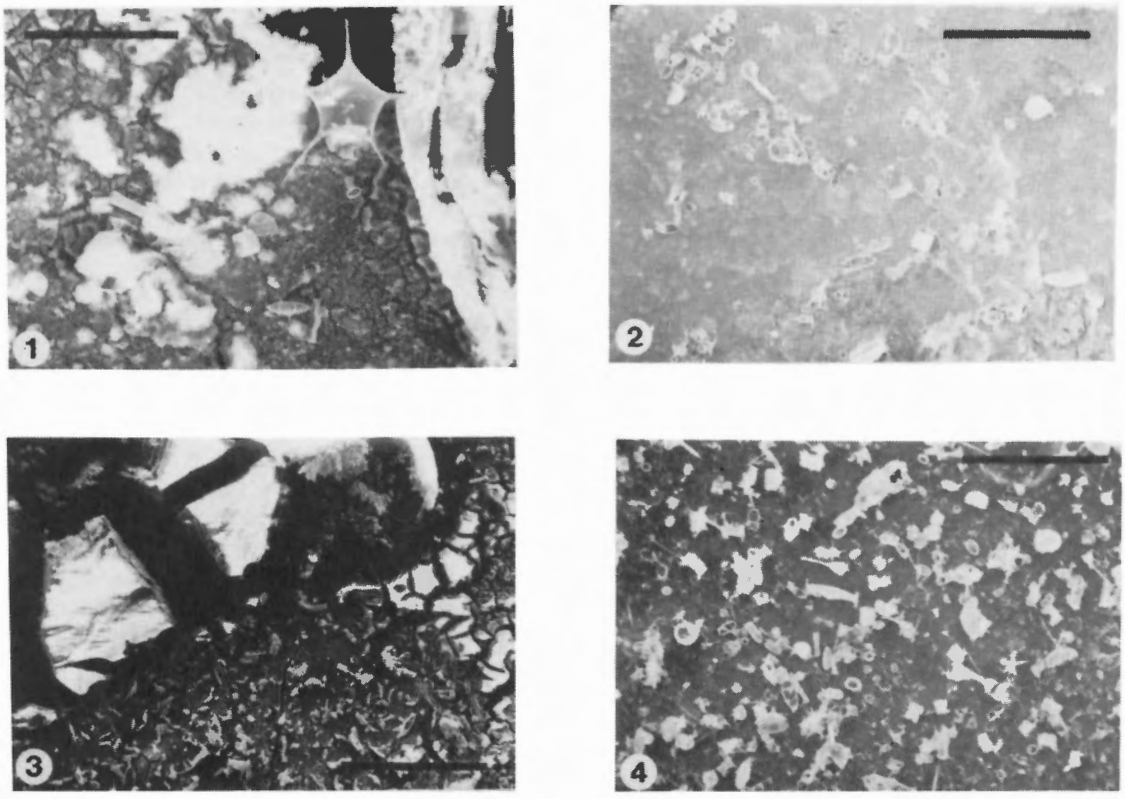

Plate 6.9

Scanning electron microscope (SEM) photographs of minerals and siliceous microfossils from laminae between 205 and 211cm depth in CESAR 6. SEM photos by B. Deonarine, AGC.

Figure 1 Suspended particulate material (SPM) from a white lamina at 207cm, showing a bone fragment, large fluffy white flocs of biogenic silica, and the wide size range of siliceous microfossils. AGC # 1138.6; bar = 100μm.

Figure 2 and 3 SPM from a brown lamina at 206.5cm. Figure 2: fine fraction, showing numerous medium to small-sized diatoms or resting spores in a filmy layer of Fe-rich flocs with traces of Al. Figure 3: coarse fraction, showing large and small particles of $CaPO_4$ and numerous medium to small diatoms or silica particles. AGC # 1137.11; bar = 300μm.

Figure 4 SPM fine fraction from a very light brown lamina at 205cm, showing abundant diatom frustules of various shapes and sizes, and common rod-shaped silica particles. AGC # 1136.15; bar = 100μm.

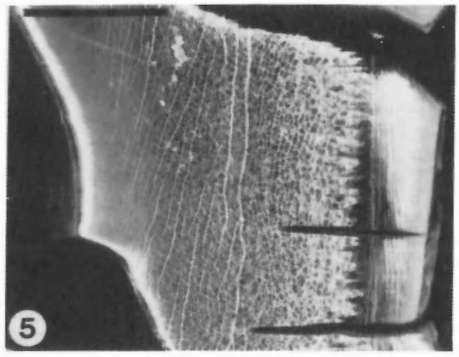

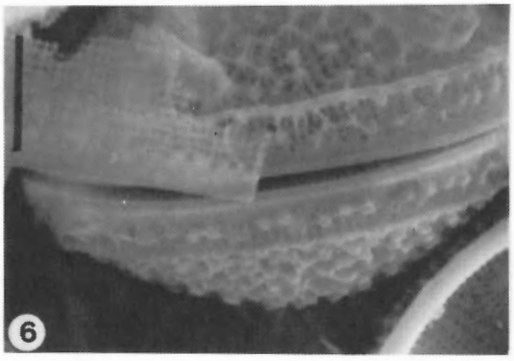

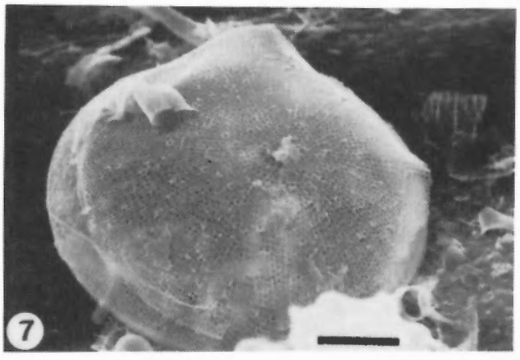

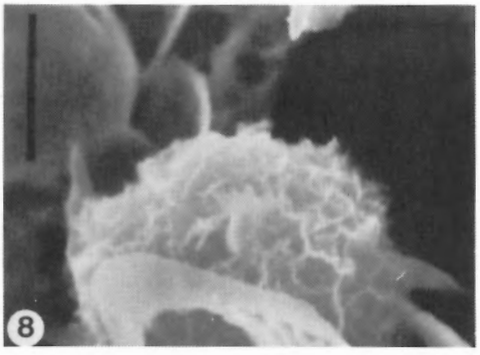

Plate 6.9 (cont'd)

Figure 5 Well-preserved bone fragment from an olive-brown lamina at 206.5cm. AGC # 1137.17; bar = 100μm.

Figure 6, 7 and 8 Diatoms from a set of light brown to white microlaminae from 209-211.5cm. Figure 6: lateral view of a diatom resting spore (?*Goniothecium* sp.) showing the excellent preservation of small diatoms. AGC # 1139.7; bar = 5μm. Figure 7: oblique surface view of *Coscinodiscus lineatus*, showing a thin patchy film of silica. AGC # 1139.3; bar = 10μm. Figure 8: frustule of *Hemiaulus* sp., showing overgrowth of MnO_2. AGC # 1139.1; bar = 3μm.

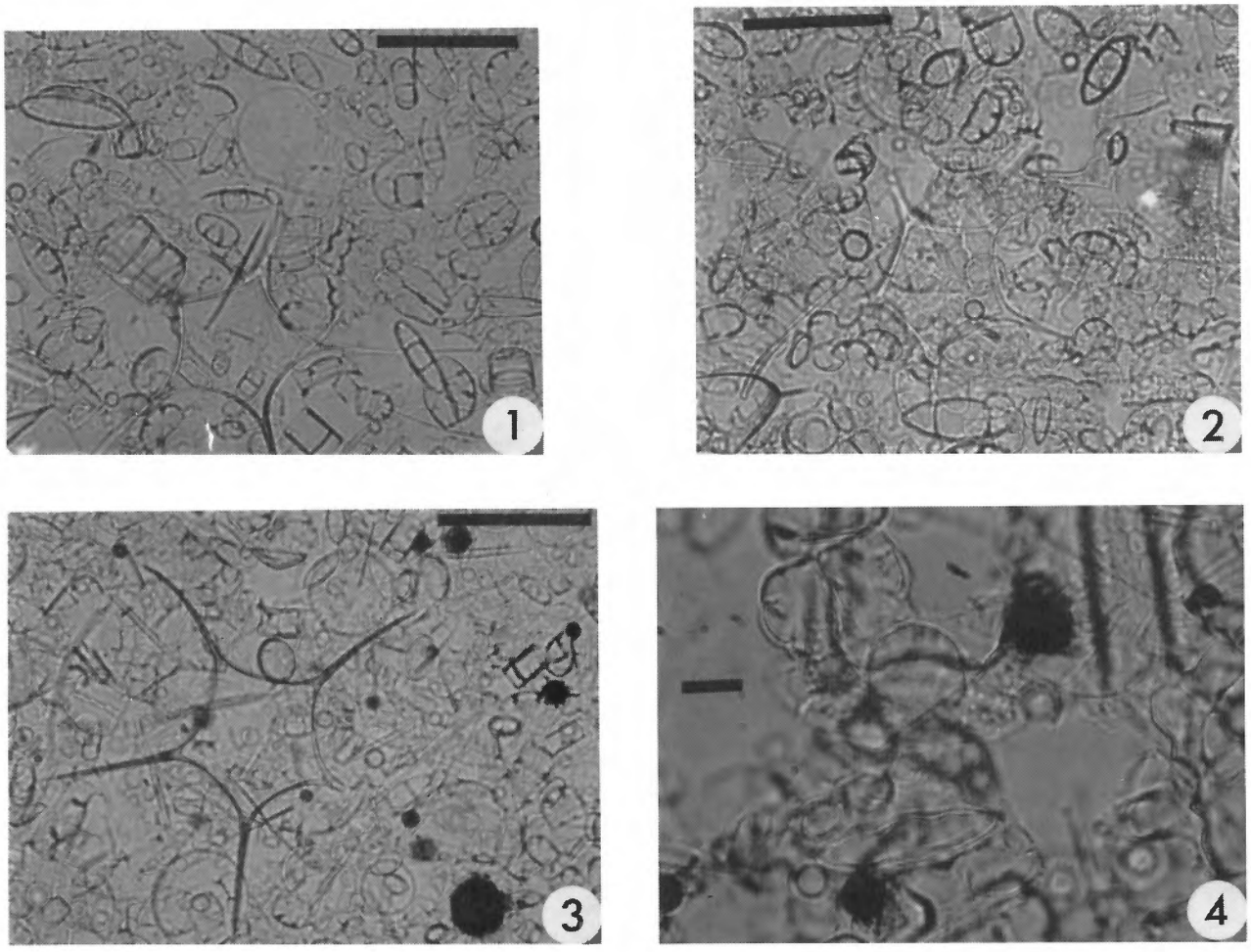

Plate 6.10

Smear slide samples of sediment from light and dark laminae, CESAR 6. Light photomicrographs; magnification × 400 except for Figure 4, 7 and 8 which are × 1000; bar scale = 50μm. Photographs by P.J. Mudie, AGC.

Figure 1 White lamina at 214.3cm, showing *Vallacerta siderea* and various diatoms, and near-absence of clay-sized particulates. Photo # 840126.12.

Figure 2 Pale brown lamina at 214cm, unburrowed area, showing *Vallacerta siderea, Lyramula burchardae* and various diatoms in a matrix of silt – clay sized particles. Photo # 840126.14.

Figure 3 Sediment from black "micronodule" at 214cm, showing *Vallacerta siderea*, numerous small diatoms and scattered black FeMn-rich pariculates. Photo # 840126.03.

Figure 4 Enlargement (× 1000) of small "micronodule" and diatom spores shown in figure 3. Photo # 840126.04.

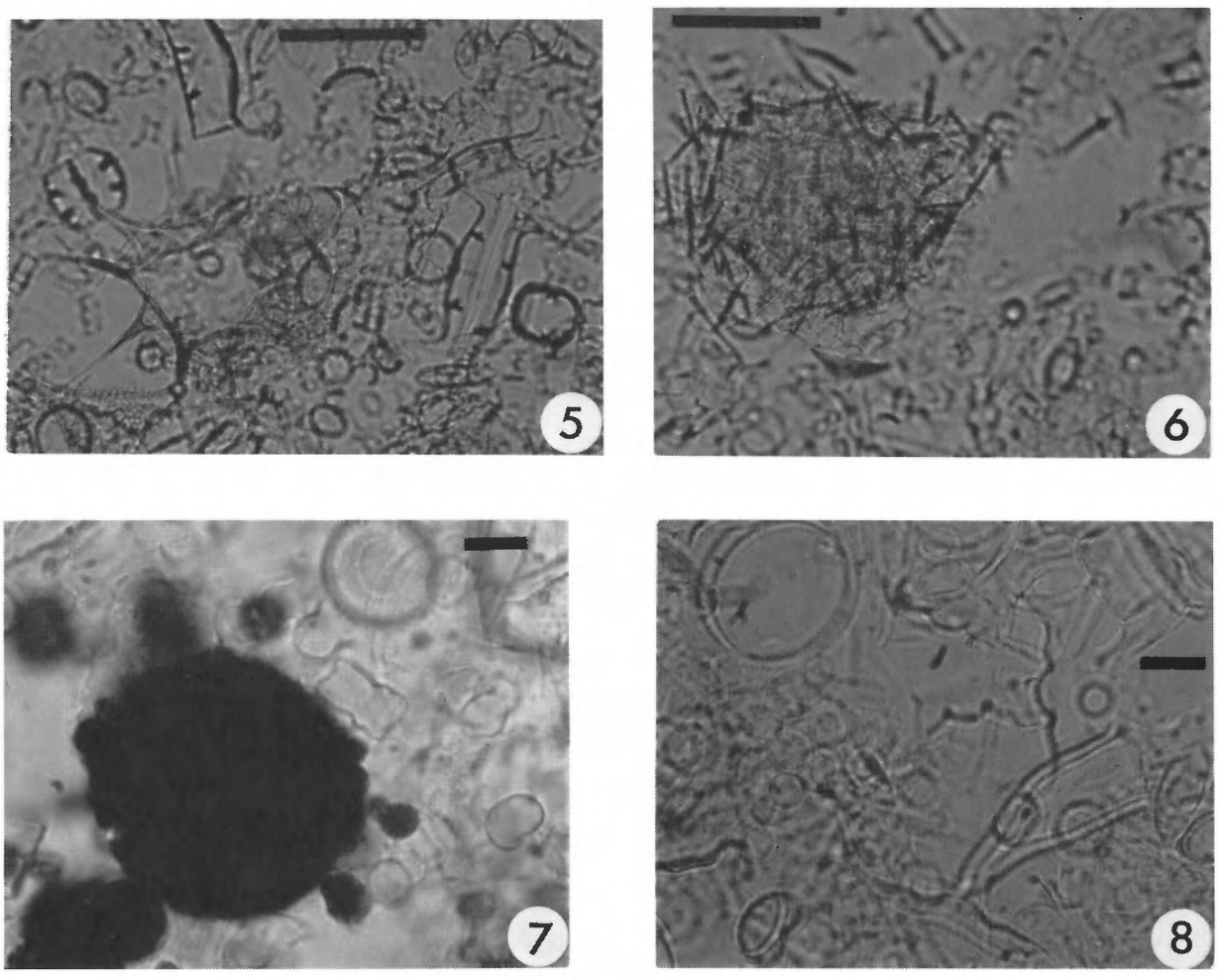

Plate 6.10 (cont'd)

Figure 5 Darker brown lamina at 213.7cm, showing general similarity to lighter laminae shown in figure 1 and 2. Photo # 840126.13.

Figure 6 White lamina at 226cm, showing "floc" containing abundant biosiliceous spicules and background of abundant small diatoms. Photo # 840126.08.

Figure 7 Enlargement (× 1000) of FeMn-rich particulates from a dark brown "micronodule" in the white lamina at 226cm. Photo # 840126.10.

Figure 8 Enlargement (× 1000) of small diatoms and resting spores in background of Figure 6. Photo # 840126.02.

REFERENCES

Aksu, A.E.
1983: Holocene and Pleistocene dissolution cycles in deep-sea cores of Baffin Bay and Davis Strait; paleoceanographic implications; Marine Geology, v.53, p.331-348.

1985a: Paleomagnetic stratigraphy of the CESAR cores; *in* Initial Geological Report on CESAR — the Canadian Expedition to Study the Alpha Ridge, Arctic Ocean, ed. H.R. Jackson, P.J. Mudie and S.M. Blasco; Geological Survey of Canada, Paper 84-22, report 7.

1985b: Planktonic foraminiferal and oxygen isotopic stratigraphy of CESAR cores 102 and 103: preliminary results; *in* Initial Geological Report on CESAR — the Canadian Expedition to Study the Alpha Ridge, Arctic Ocean, ed. H.R. Jackson, P.J. Mudie and S.M. Blasco; Geological Survey of Canada, Paper 84-22, report 8.

Barron, J.A.
1985: Diatom biostratigraphy of the CESAR 6 core; *in* Initial Geological Report on CESAR — the Canadian Expedition to Study the Alpha Ridge, Arctic Ocean, ed. H.R. Jackson, P.J. Mudie and S.M. Blasco; Geological Survey of Canada, Paper 84-22, report 10.

Berger, W.H. and Roth, P.H.
1975: Oceanic micropaleontology; progress and prospect; Reviews of Geophysics and Space Physics, v.13, p.561-636.

Berger, W.H. and Winterer, E.L.
1974: Plate stratigraphy and the fluctuating carbonate line; *in* Pelagic Sediments on Land and Under the Sea: ed. K.J. Hsü and J.C. Jenkyns; Special Publication No. 1 of the International Association of Sedimentologists, p.11-48, Blackwell Scientific Publications, Oxford.

Blasco, S.M., Bornhold, B.D., and Lewis, C.F.M.
1979: Preliminary results of surficial geology and geomorphology studies of the Lomonosov Ridge, central Arctic Basin; *in* Current Research, Part C, Geological Survey of Canada, Paper 79-1C, p.73-83.

Bukry, D.
1981: Cretaceous arctic silicoflagellates; Geo-Marine Letters, v.1, p.57-63.

Bukry D.
1985: Correlation of Late Cretaceous silicoflagellates from Alpha Ridge; *in* Initial Geological Report on CESAR — the Canadian Expedition to Study the Alpha Ridge, Arctic Ocean, ed. H.R. Jackson, P.J. Mudie and S.M. Blasco; Geological Survey of Canada, Paper 84-22, report 9.

Clark, D.L.
1977: Climatic factors of the Late Mesozoic and Cenozoic Arctic Ocean; *in* Polar Oceans, ed. M.J. Dunbar; Arctic Institute of North America, Calgary, Alberta, p.603-613.

1982: Origin, nature and world climate effect of Arctic Ocean ice-cover; Nature, v.300, p.321-325.

Clark, D.L., Whitman, R.R., Morgan, K.A., and Mackey, S.D.
1980: Stratigraphy and glacial-marine sediments of the Amerasian Basin, central Arctic Ocean; Geological Society of America, Special Paper 181, 57p.

Harland, W.B., Cox, A.V., Llewellyn, P.G., Pickton, C.A.G., Smith, A.G., and Walters, R.
1982: A Geological Time Scale; Cambridge University Press, Cambridge, U.K., 131p.

Heezen, B.C. and Hollister, C.D.
1971: The Face of the Deep; Oxford University Press, New York, 659p.

Hein, J.R. and Karl, S.M.
1983: Comparisons between open-ocean and continental margin chert sequences; *in* Siliceous Deposits in the Pacific Region, ed. A. Iijima, J.R. Hein and R. Siever; Developments in Sedimentology, v.36, Elsevier Scientific Publishing Co., Amsterdam, p.25-43.

Herman, Y.
1974: Arctic Ocean sediments, microfauna, and the climatic record in Late Cenozoic time; *in* Marine Geology and Oceanography of the Arctic Seas, ed. Y. Herman; Springer-Verlag, New York, p.283-348.

1983: Baffin Bay; present-day analog of the central Arctic during Late Pliocene and mid-Pleistocene time; Geology, v.11, p.356-359.

Iijima, A. and Utada, M.
1983: Recent developments in the sedimentology of siliceous deposits in Japan; *in* Siliceous Deposits in the Pacific Region, ed. A. Iijima, J.R. Hein and R. Siever; Developments in Sedimentology, v.36, p.45-64.

Isaacs, C.M.
1981: Porosity reduction during diagenesis of the Monterey Formation, Santa Barbara coastal area, California; *in* The Monterey Formation and Related Siliceous Rocks of California, ed. R.E. Garrison et al.; Special Paper of the Society of Economic Paleontologists and Mineralogists, p.257-271.

Jackson, H.R.
1985: Seismic reflection results from CESAR; *in* Initial Geological Report on CESAR — the Canadian Expedition to Study the Alpha Ridge, Arctic Ocean, ed. H.R. Jackson, P.J. Mudie and S.M. Blasco; Geological Survey of Canada, Paper 84-22, report 3.

Jodrey, F. and Heffler, D.
1985: Piston coring on CESAR; *in* Initial Geological Report on CESAR — the Canadian Expedition to Study the Alpha Ridge, Arctic Ocean, ed. H.R. Jackson, P.J. Mudie and S.M. Blasco; Geological Survey of Canada, Paper 84-22, report 12.

Kitchell, J.A. and Clark, D.L.
1982: Late Cretaceous-Paleozoic paleogeography and paleocirculation; evidence of North Polar upwelling; Paleogeography, Paleoclimatology, Paleoecology, v.40, p.135-165.

Marincovich, L., Brouwers, E.M., and Hopkins, D.M.
1983: Paleogeographic affinities and endemism of Cretaceous and Paleogene marine faunas in the Arctic; U.S. Geological Survey Polar Research Symposium, Abstracts with Program, p.45-46; Geological Survey Circular 911.

Miall, A.D.
1979: Mesozoic and Tertiary geology of Banks Island, Arctic Canada; The history of an unstable craton margin; Geological Survey of Canada, Memoir 387, 235p.

Minicucci, D.A. and Clark, D.L.
1983: A Late Cenozoic stratigraphy for glacial-marine sediments of the eastern Alpha Cordillera, central Arctic Ocean; *in* Glacial-marine Sedimentation, ed. B.F. Molnia; Plenum Publishing Corp., New York and London, p.331-365.

Mudie, P.J.and Aksu, A.E.
1984: Paleoclimate of Baffin Bay: 300 000 yr. record of foraminifera, dinoflagellates and pollen; Nature, v. 312, p. 630-634.

Mudie, P.J., Piper, D.J.W., Rideout, K., Robertson, K.R., Schafer, C.T., Vilks, G., and Hardy, I.A.
1984: Standard methods for collecting, describing and sampling Quaternary sediments at the Atlantic Geoscience Centre; Geological Survey of Canada, Open File 1044, 39 p.

Mudie, P.J.
1985: Palynology of the CESAR cores, Alpha Ridge; *in* Initial Geological Report on CESAR — the Canadian Expedition to Study the Alpha Ridge, Arctic Ocean, ed. H.R. Jackson, P.J. Mudie and S.M. Blasco; Geological Survey of Canada, Paper 84-22, report 11.

Nisbet, E.G. and Price, I.
1974: Siliceous turbidites: bedded chert as redeposited, ocean ridge-derived sediments; *in* Pelagic Sediments; On Land and Under the Sea, ed. K.J. Hsu and H.C. Jenkyns; Special Publications of the International Association of Sedimentologists, v.1, p.351-366.

Plauchut, B.P. and Jutard, G.G.
1976: Cretaceous and Tertiary stratigraphy, Banks and Eglinton islands and Anderson Plain (N.W.T.); Bulletin of Canadian Petroleum Geology, v.24, p.321-371.

Schnitker, D., Mayer, L.M., and Norton, S.
1980: Loss of calcareous fossils from sediments through gypsum formation; Marine Geology, v.36, p.M35-M44.

Siever, R.
1983: Evolution of chert at active and passive continental margins; *in* Siliceous Deposits in the Pacific Region, ed. A. Iijima, J.R. Hein and R. Siever; Developments in Sedimentology, v.36, p.7-24, Elsevier Scientific Publishing Co., Amsterdam.

Soutar, A., Johnson, S.R., and Taylor, E.
1982: X-radiography of Hole 480, procedures and results: Initial Reports of the Deep Sea Drilling Project, v.64, part 2, U.S. Government Printing Office, Washington, p. 1183-1190.

Thiede, J., Dean, W.E., and Claypool, G.E.
1982: Oxygen-deficient depositional paleoenvironments in the mid-Cretaceous tropical and subtropical Pacific Oceans; *in* Nature and Origin of Cretaceous Carbon-Rich Facies, ed. S.O. Schlanger and M.B. Cita; Academic Press, London and New York, p.79-100.

Vincent, J.S., Ochietti, S., Rutter, N., Lortie, G., Gilbault, J.P., and De Boutray, B.
1983: The Late Tertiary-Quaternary stratigraphic record of the Duck Hawk Bluffs, Banks Island, Canadian Arctic Archipelago; Canadian Journal of Earth Sciences, v.20, p.1694-1712.